

Phase Portraits of general $f(T)$ Cosmology

A. Awad^{a,b} W. El Hanafy^{c,d} G.G.L. Nashed^{c,d,e} Emmanuel N. Saridakis^{f,g,h}

^a*Department of Physics, School of Sciences and Engineering, American University in Cairo, P.O. Box 74, AUC Avenue New Cairo, Cairo, Egypt*

^b*Physics Department, Faculty of Science, Ain Shams University, Cairo 11566, Egypt*

^c*Centre for Theoretical Physics, the British University in Egypt, P.O. Box 43, El Sherouk City, Cairo 11837, Egypt*

^d*Egyptian Relativity Group (ERG), Cairo University, Giza 12613, Egypt*

^e*Mathematics Department, Faculty of Science, Ain Shams University, Cairo 11566, Egypt*

^f*Chongqing University of Posts & Telecommunications, Chongqing, 400065, China*

^g*Department of Physics, National Technical University of Athens, Zografou Campus GR 157 73, Athens, Greece*

^h*CASPER, Physics Department, Baylor University, Waco, TX 76798-7310, USA*

E-mail: adel.awad@bue.edu.eg, waleed.elhanafy@bue.edu.eg, nashed@bue.edu.eg, Emmanuel.Saridakis@baylor.edu

ABSTRACT: We use dynamical system methods to explore the general behaviour of $f(T)$ cosmology. In contrast to the standard applications of dynamical analysis, we present a way to transform the equations into a one-dimensional autonomous system, taking advantage of the crucial property that the torsion scalar in flat FRW geometry is just a function of the Hubble function, thus the field equations include only up to first derivatives of it, and therefore in a general $f(T)$ cosmological scenario every quantity is expressed only in terms of the Hubble function. The great advantage is that for one-dimensional systems it is easy to construct the phase space portraits, and thus extract information and explore in detail the features and possible behaviours of $f(T)$ cosmology. We utilize the phase space portraits and we show that $f(T)$ cosmology can describe the universe evolution in agreement with observations, namely starting from a Big Bang singularity, evolving into the subsequent thermal history and the matter domination, entering into a late-time accelerated expansion, and resulting to the de Sitter phase in the far future. Nevertheless, $f(T)$ cosmology can present a rich class of more exotic behaviours, such as the cosmological bounce and turnaround, the phantom-divide crossing, the Big Brake and the Big Crunch, and it may exhibit various singularities, including the non-harmful ones of type II and type IV. We study the phase space of three specific viable $f(T)$ models offering a complete picture. Moreover, we present a new model of $f(T)$ gravity that can lead to a universe in agreement with observations, free of perturbative instabilities, and applying the $\text{Om}(z)$ diagnostic test we confirm that it is in agreement with the combination of SNIa, BAO and CMB data at 1σ confidence level.

KEYWORDS: $f(T)$ gravity, dynamical systems, dark energy, cosmological bounce, cosmological singularities

Contents

1	Introduction	1
2	$f(T)$ gravity and cosmology	4
3	General features of cosmological phase portraits of $f(T)$ cosmology	7
3.1	Flow, fixed points and stability	7
3.2	Phase portraits of standard cosmological evolution	10
3.2.1	Fixed effective equation of state	10
3.2.2	Dynamical effective equation of state	12
3.3	Phase portraits of finite-time singularities of Type II and IV	14
3.3.1	Non-singular bounce	14
3.3.2	Singular bounce	16
4	Cosmological phase portraits of specific $f(T)$ models	17
4.1	f_1 CDM model: $f(T) = T + \alpha(-T)^b$	17
4.2	f_2 CDM model: $f(T) = T + \alpha T_0 \left(1 - e^{-p\sqrt{T/T_0}}\right)$	19
4.3	f_3 CDM model: $f(T) = T + \alpha T_0 \left(1 - e^{-pT/T_0}\right)$	21
5	A new viable $f(T)$ model	22
5.1	The model: $f(T) = T e^{\beta T_0/T}$	23
5.2	Phase space portraits	23
5.3	Cosmological evolution	25
5.4	Two diagnostic tests	28
6	Conclusions	29

1 Introduction

Current astrophysical and cosmological observations are essential to consummate and sharpen our knowledge of the fundamental constituents of the universe. Cosmic microwave background (CMB) anisotropies observations provides us with a substantial information on the physics of the primordial universe, which is essential in understanding, as well as constraining, physical models explaining early-time cosmology. The CMB anisotropies have been measured by COBE, WMAP and Planck satellites with high precisions [1–5]. The observations have shown that baryonic matter constitutes only a small portion ($\sim 5\%$) of the universe’s energy content. However, observations of the rotation galaxy curves [6], galaxy clustering [7] and galaxy X-ray emission [8] have shown that $\sim 26\%$ of the universe’s total energy is dark matter. Dark matter is needed for forming clusters and large scale structures early enough, since baryonic matter alone cannot explain the existence of

these structures at high redshifts. On the other hand, the luminosity distance observations [9, 10] of type Ia supernovae (SNIa), affirmed by CMB observations [2–5], have come up with another unexpected result, namely that the cosmic expansion has passed from deceleration to acceleration a few billion years ago, i.e at redshift $z_{tr} \sim 0.6 - 0.8$ [11]. Since none of the known matter fields can explain this accelerated expansion, cosmologists have assumed new obscure cosmic species, that are collectively called dark energy, to explain it. This component represents $\sim 69\%$ of the universe’s total energy.

The simplest and basic scenario which incorporates the dark energy component is a cosmological constant (Λ) universe. With the addition of cold dark matter (CDM) and the consideration of a flat Friedmann-Robertson-Walker (FRW) geometry (since the spatial flat geometry gives a good agreement with temperature power spectrum of Planck observations), this scenario is the so-called Λ CDM one. Although the Λ CDM paradigm is the one that fits the data in the most efficient way, the possibility of the dynamical nature of the dark energy component, as well as possible tensions relating to the direct observations of the Hubble function [12–14], might indicate towards dynamical dark energy models, unless unknown uncertainties will be discovered [15, 16]. Dynamical dark energy models could explain the late accelerated expansion by introducing various extra fields (for reviews see [17, 18]), or by assuming fluids with exotic equation of state, such as the Chaplygin fluid.

On the other hand, modified gravity may provide an alternative approach to interpret the accelerated expansion. In particular, one wishes to construct a gravitational modification, that includes extra degrees of freedom that can drive the universe acceleration, at early or late times, which however still possesses general relativity as a particular limit. Although most of the works in modified gravity start from the standard curvature-based formulation (for reviews see [19, 20]), one can alternatively construct modified gravities based on torsion [21]. In particular, starting from the Teleparallel Equivalent of General Relativity (TEGR) [22], in which the Lagrangian is the torsion scalar T , one can extend T to $f(T)$ resulting to $f(T)$ gravity [23, 24]. Note that although TEGR is completely equivalent with general relativity at the level of equations, $f(T)$ gravity is different from $f(R)$ gravity. Thus, $f(T)$ cosmology proves to be very interesting both for early-time [25–28] as well as late-time [29–83] universe evolution, while the black hole solutions in this framework also lead to interesting features [84–100].

One of the important features of both general relativity, as well as modified gravity, is that the highly nonlinear nature of the corresponding cosmological equations in general does not allow for the extraction of analytical solutions. Nevertheless, one can apply the dynamical systems method [101–104] which allows to extract the global behaviour of the scenario, independently of the initial conditions and bypassing the complexity of the equations. The dynamical systems method serves as an important tool to describe, analyze and classify various features of cosmological models, and additionally it makes more transparent the relation between different branches of solutions. In particular, in cosmological applications we are interested in the following set of ordinary differential equations

$$\frac{d\mathbf{x}}{dt} = \mathbf{f}(\mathbf{x}), \quad (1.1)$$

where $\mathbf{x} = (x_1, \dots, x_n)$ are the variables needed to characterize the system and the functions $\mathbf{f}(\mathbf{x}) = (f_1(x_1, \dots, x_n), \dots, f_n(x_1, \dots, x_n))$ are determined by the system. In general, in most nonlinear

systems analytical solutions cannot be extracted. When there is no explicit dependence of $\mathbf{f}(\mathbf{x})$ on t , the system is *autonomous*, and then the geometric approach which has been developed is applied in order to study the qualitative behaviour and the stability. In this framework one uses topological and geometrical procedures in order to determine the properties of the set of all solutions, by visualizing it as *trajectories* in a *phase space*. In this sense, the phase of the system at instant time can be described by a *phase vector* $\mathbf{x} \in \mathbf{X} \subseteq \mathbb{R}^n$, where \mathbf{X} is an n -dimensional phase space and the maps $\mathbf{f} : \mathbf{X} \rightarrow \mathbf{X}$ are *vector fields* on \mathbb{R}^n . Hence, one visualizes the phase space with frozen trajectories on it, and by using geometrical reasoning he can extract essential information about the system even without solving it explicitly.

In general applications of dynamical system methods in given cosmological scenarios, one results to a multi-dimensional system that needs to be investigated [104–111]. Analyzing multi-dimensional autonomous systems can be a complicated task, since they incorporate a large amount of information, with many solution branches and possible behaviours. However, $f(T)$ cosmology is a very interesting exception, since in a flat FRW geometry its corresponding dynamical system (1.1) can be reduced to a *one-dimensional (or first order) autonomous system*, i.e having $n = 1$. The reason behind this crucial and very helpful property is the special feature of $f(T)$ gravity, namely that the torsion scalar in flat FRW geometry is just $T = -6H^2$, i.e it can be used interchangeably with the Hubble function H (in turn this is a result from the most general feature of $f(T)$ gravity, namely that it has second-order field equations, in contrast with most models of modified gravity which include higher-order field equations). Hence, a general $f(T)$ cosmological scenario can be described by a one-dimensional autonomous system, where everything is expressed in terms of the Hubble function, and thus its possible behaviours can be extracted and investigated in huge detail.

In the present work we are interested in using the above property of $f(T)$ cosmology to transform the cosmological equations into a one-dimensional autonomous system, and then explore its features in general. We mention here that the phase space analysis of $f(T)$ cosmology has been performed in the literature [112–118], however it was based on the usual approach and thus it was performed only for particular specific $f(T)$ models (see also [119, 120], where a general analysis is performed but in the framework of multi-dimensional systems). On the other hand, in the present work, due to the above formalism, we are able to explore the phase space portraits in full detail and for general $f(T)$ cosmology. After this general analysis, we proceed to the investigation of specific viable $f(T)$ models, reproducing the results of the literature, providing a unified and full picture of $f(T)$ cosmology.

We organize the manuscript as follows: In Sec. 2, we review briefly the essential background of $f(T)$ gravity, and we apply it in a cosmological framework. In Sec. 3, we present the theory of cosmological phase portraits and we show that $f(T)$ cosmology has the crucial property to result in a one-dimensional autonomous system. Then we study the basic features of the phase portraits in general $f(T)$ cosmology. In Sec. 4, we explore the phase space portraits of three viable specific $f(T)$ models, investigating all possible cosmological evolutions. In Sec. 5, taking into account the information gained through the phase space portraits, we propose a new $f(T)$ model and we show that it can successfully describe the universe evolution in agreement with observations. Finally, in Sec. 6 we summarize the obtained results.

2 $f(T)$ gravity and cosmology

In this section we briefly review $f(T)$ gravity and we apply it in a cosmological framework. We start from a 4-dimensional smooth manifold \mathcal{M} , and we are given a set of tetrad fields $e_{a\mu}$ defined on \mathcal{M} , where the Latin letters denote the local Lorentz (tangent space) indices, and the Greek letters denote the tensor (spacetime) indices. The local Lorentz and the tensor indices can be interchanged using

$$e^a{}_\nu e_a{}^\mu = \delta_\nu^\mu, \quad e^a{}_\mu e_b{}^\mu = \delta_b^a. \quad (2.1)$$

One can construct the metric tensor

$$g_{\mu\nu} = \eta_{ab} e^a{}_\mu e^b{}_\nu, \quad (2.2)$$

where $\eta_{ab} = \text{diag}(1, -1, -1, -1)$ is the metric tensor of the tangent space. In the above manifold one can introduce the Levi-Civita connection

$$\overset{\circ}{\Gamma}{}^\alpha{}_{\mu\nu} = \frac{1}{2} g^{\alpha\sigma} (\partial_\nu g_{\mu\sigma} + \partial_\mu g_{\nu\sigma} - \partial_\sigma g_{\mu\nu}), \quad (2.3)$$

which satisfies the metricity condition $\overset{\circ}{\nabla}_\sigma g_{\mu\nu} = 0$, where the operator $\overset{\circ}{\nabla}$ denotes the covariant derivative of the Levi-Civita connection. The corresponding torsion tensor $\overset{\circ}{T}{}^\alpha{}_{\mu\nu}$ vanishes identically, since the connection $\overset{\circ}{\Gamma}{}^\alpha{}_{\mu\nu}$ is symmetric, while its curvature tensor is the usual one, namely $\overset{\circ}{R}{}^\alpha{}_{\sigma\mu\nu} = \partial_\mu \overset{\circ}{\Gamma}{}^\alpha{}_{\sigma\nu} - \partial_\nu \overset{\circ}{\Gamma}{}^\alpha{}_{\sigma\mu} + \overset{\circ}{\Gamma}{}^\alpha{}_{\lambda\mu} \overset{\circ}{\Gamma}{}^\lambda{}_{\sigma\nu} - \overset{\circ}{\Gamma}{}^\alpha{}_{\lambda\nu} \overset{\circ}{\Gamma}{}^\lambda{}_{\sigma\mu}$, and non-vanishing. As usual, in general relativity one constructs the Ricci scalar $\overset{\circ}{R}$, through contractions of this curvature tensor, and uses it as the Lagrangian that describes the gravitational field.

On the other hand, one can alternatively introduce the Weitzenböck connection, constructed directly from the tetrad fields as

$$\Gamma^\alpha{}_{\mu\nu} = e_a{}^\alpha \partial_\nu e^a{}_\mu = -e^a{}_\mu \partial_\nu e_a{}^\alpha. \quad (2.4)$$

This connection defines auto-parallelism, where the covariant derivative of the tetrad fields vanishes

$$\nabla_\sigma e^a{}_\mu = 0, \quad (2.5)$$

(∇ denotes the covariant derivative corresponding to the Weitzenböck connection), and thus we directly deduce that the Weitzenböck connection is a metric one:

$$\nabla_\sigma g_{\mu\nu} = 0. \quad (2.6)$$

The important feature of this connection is that it has vanishing curvature tensor $R^\alpha{}_{\sigma\mu\nu} = 0$, while its torsion tensor is given by

$$T^\alpha{}_{\mu\nu} = \Gamma^\alpha{}_{\nu\mu} - \Gamma^\alpha{}_{\mu\nu} = e_a{}^\alpha (\partial_\mu e^a{}_\nu - \partial_\nu e^a{}_\mu). \quad (2.7)$$

Additionally, we can define the contortion tensor $K^\alpha{}_{\mu\nu} = \Gamma^\alpha{}_{\mu\nu} - \overset{\circ}{\Gamma}{}^\alpha{}_{\mu\nu} = e_a{}^\alpha \overset{\circ}{\nabla}_\nu e^a{}_\mu$, which can be expressed as

$$K^\alpha{}_{\mu\nu} = \frac{1}{2} (T_\mu{}^\alpha{}_\nu + T_\nu{}^\alpha{}_\mu - T^\alpha{}_{\mu\nu}). \quad (2.8)$$

Using contractions of the torsion tensor one can construct the teleparallel torsion scalar as

$$T = \frac{1}{4}T^\alpha{}_{\mu\nu}T^\alpha{}^{\mu\nu} + \frac{1}{2}T^\alpha{}_{\mu\nu}T^{\nu\mu}{}_\alpha - T_\mu T^\mu \equiv S_\alpha{}^{\mu\nu}T^\alpha{}_{\mu\nu}, \quad (2.9)$$

where for convenience we have introduced the superpotential

$$S_\alpha{}^{\mu\nu} = \frac{1}{4}(T_\alpha{}^{\mu\nu} + T^\mu{}_\alpha{}^\nu - T^\nu{}_\alpha{}^\mu) + \frac{1}{2}(\delta_\alpha^\nu T^\mu - \delta_\alpha^\mu T^\nu), \quad (2.10)$$

which is skew symmetric in the last pair of indices. One can straightforwardly see that

$$e\overset{\circ}{R} \equiv -eT + 2\partial_\mu(eT^\mu), \quad (2.11)$$

with $e = \sqrt{-g} = \det(e^a{}_\mu)$, and thus when T is used as a gravitational Lagrangian it will lead to the same equations with the use of the Ricci scalar $\overset{\circ}{R}$. That is why the torsional theory characterized by the action

$$\mathcal{S}_{TEGR} = \frac{1}{2\kappa^2} \int d^4x e(T + \Lambda), \quad (2.12)$$

with $\kappa^2 = 8\pi G$ and Λ a (cosmological) constant, is called Teleparallel Equivalent of General Relativity (TEGR).

One can be inspired by the $f(\overset{\circ}{R})$ extensions of the Einstein-Hilbert action, and extend T to $f(T)$, i.e use the action [21]

$$\mathcal{S} = \int d^4x e \left[\frac{1}{2\kappa^2} f(T) \right], \quad (2.13)$$

resulting to the $f(T)$ gravity. Adding also the action for the matter sector, and varying the action with respect to the vierbein, gives rise to the field equations, namely [121, 122]

$$\frac{1}{e}\partial_\mu(eS_a{}^{\mu\nu})f_T - e_a^\lambda T^\rho{}_{\mu\lambda} S_\rho{}^{\nu\mu} f_T + S_a{}^{\mu\nu} \partial_\mu T f_{TT} + \frac{1}{4}e_a^\nu f(T) = \frac{\kappa^2}{2}e_a^\mu \mathfrak{T}_\mu{}^\nu, \quad (2.14)$$

with $f_T := \frac{df}{dT}$ and $f_{TT} := \frac{d^2f}{dT^2}$, and where $\mathfrak{T}_\mu{}^\nu = e^a{}_\mu \left(-\frac{1}{e} \frac{\delta \mathcal{L}_m}{\delta e^a{}_\nu} \right)$ is the energy-momentum tensor of the matter fields.

$f(T)$ gravity exhibits interesting properties. In particular, through a Hamiltonian analysis one can show that in D spacetime dimensions it has $D - 1$ extra degrees of freedom, corresponding to one massive vector field or one massless vector field with one scalar field [123]. Furthermore, although the theory has second-order field equations at the background level, at the perurbation level instabilities could arise, and thus one must impose specific conditions for the absence of ghost and Laplacian instabilities [29, 35].

In order to apply $f(T)$ gravity in a cosmological framework we impose the homogeneous and isotropic geometry

$$e_\mu{}^a = \text{diag}(1, a(t), a(t), a(t)), \quad (2.15)$$

which corresponds to the flat Friedmann-Robertson-Walker (FRW) metric

$$ds^2 = dt^2 - a^2(t) \delta_{ij} dx^i dx^j, \quad (2.16)$$

where $a(t)$ is the scale factor. Calculating the torsion scalar T from (2.9) for the vierbein choice (2.15), gives

$$T = -6H^2, \quad (2.17)$$

where $H \equiv \dot{a}/a$ is the Hubble function and dots denote derivative with respect to t . Hence, in $f(T)$ gravity there is a relation that directly relates T (whose arbitrary function is the Lagrangian of the theory) to H . As we mentioned in the Introduction, this relation is crucial for the present work.

Inserting the vierbein choice (2.15) into the general field equations (2.14), we acquire the two modified Friedmann equations, namely

$$H^2 = \frac{\kappa^2}{3}(\rho + \rho_T), \quad (2.18)$$

$$2\dot{H} + 3H^2 = -\kappa^2(p + p_T), \quad (2.19)$$

where ρ and p are respectively the energy density and pressure of the matter sector, considered to correspond to a perfect fluid with equation-of-state parameter $w \equiv p/\rho$. In the above expressions we have defined

$$\rho_T = \frac{1}{2\kappa^2} [2Tf_T - T - f(T)], \quad (2.20)$$

$$p_T = \frac{1}{2\kappa^2} \left[\frac{f(T) - Tf_T + 2T^2 f_{TT}}{f_T + 2Tf_{TT}} \right], \quad (2.21)$$

i.e ρ_T and p_T incorporate the effects of torsional modifications. The equations close by considering the standard matter conservation equation

$$\dot{\rho} + 3H(\rho + p) = 0, \quad (2.22)$$

in which case one obtains additionally the conservation equation of the torsional fluid, namely

$$\dot{\rho}_T + 3H(\rho_T + p_T) = 0, \quad (2.23)$$

while its equation-of-state parameter is $w_T \equiv p_T/\rho_T$. If the above formulation is applied at late times, then this torsional fluid will constitute the dark energy sector with equation-of-state parameter

$$w_{DE} \equiv w_T = \frac{p_T}{\rho_T} = -1 + \frac{[f(T) - 2Tf_T](f_T + 2Tf_{TT} - 1)}{[f(T) + T - 2Tf_T](f_T + 2Tf_{TT})}. \quad (2.24)$$

Finally, it proves convenient to define the effective, i.e the total, fluid of the universe through

$$\rho_{eff} \equiv \rho + \rho_T \quad (2.25)$$

$$p_{eff} = p + p_T, \quad (2.26)$$

as well as the effective equation-of-state parameter

$$w_{eff} \equiv \frac{p_{eff}}{\rho_{eff}} = -1 - \frac{2}{3} \frac{\dot{H}}{H^2}, \quad (2.27)$$

where the last equality arises straightforwardly from the Friedmann equations (2.18), (2.19). This effective equation-of-state parameter is useful since it is straightforwardly related to the deceleration parameter

$$q \equiv -1 - \frac{\dot{H}}{H^2} = \frac{1 + 3w_{eff}}{2}. \quad (2.28)$$

3 General features of cosmological phase portraits of $f(T)$ cosmology

In this section we investigate the general phase space portraits and the behaviour of general $f(T)$ cosmology. In order to perform this analysis we take advantage of the special property of $f(T)$ cosmology that the torsion scalar T can be expressed as a quadratic function of the Hubble function, namely relation (2.17). Hence, both torsional energy density and pressure, given in (2.20), (2.21) are functions of H , and then from the first Friedmann equation (2.18) we deduce that the matter energy density ρ can also be expressed as a function of H . Thus, for a barotropic fluid with $p = p(\rho)$ the pressure is also a function of H , and then from the second Friedmann equation (2.19) it is implied that \dot{H} is a function of H too, as well as w_{eff} through (2.27). This feature, namely that \dot{H} in $f(T)$ cosmology can be expressed as a function of H , namely

$$\dot{H} = \mathcal{F}(H), \quad (3.1)$$

is central in the present work, and it allows for the reduction of the cosmological equations into a one-dimensional autonomous system, which can be explored in detail. Finally, from the conservation equation (2.22), taking into account the above features, we deduce that for a barotropic fluid the scale factor itself can be expressed as a function of H .

In summary, in $f(T)$ cosmology in a flat FRW universe every quantity can be expressed as a function of the Hubble function H , which allows for the use of one-dimensional autonomous system methods (note that in case of non-flat geometry the various quantities would have an additional explicit dependence on the scale factor, e.g $\dot{H} = \mathcal{F}(H, a(t))$, which is a non-autonomous system and thus the present methods could not be used).

3.1 Flow, fixed points and stability

We can interpret the differential equation (3.1) as a vector field on a line, introducing one of the basic techniques of dynamical analysis. In this view, we can draw the phase space diagram of H , namely draw \dot{H} versus H , which is the basic tool to analyze the cosmic evolution in a clear and transparent way, without the need to know exact analytic solutions. For clarity, in Fig. 1 we present a toy-example of such a portrait, since portraits like this will be used extensively in the following. In this framework, one focuses on two features of this analysis, which constitute a complete description of the evolution of H as a function of time.

The first feature is the evolution/flow of the vector field H , which is represented by an arrow showing the direction of the change of H along the x-axis. This is determined from the sign of \dot{H} , since a small change in H is given by $\delta H = \mathcal{F}(H)\delta t$. In other words, if $\mathcal{F}(H) > 0$ then H flows towards the right (increasing) direction as time t increases. On the contrary, if $\mathcal{F}(H) < 0$ then H flows towards the left (decreasing) direction as time increases.

The second feature is the existence of fixed points or singularities which terminate the flow. In particular, solutions of the first-order differential equation $\dot{H} = \mathcal{F}(H)$ are subject to the initial conditions $H(t_i) = H_i$ at $t = t_i$ and can be divided into different branches, if the equation has fixed points. The fixed points are the zero's of $\mathcal{F}(H)$, which are just de Sitter solutions, since at these points the Hubble parameter $H = H^*$ is constant and $\dot{H} = 0$. If the flow starts from a fixed point, it will remain eternally at this point, that is the universe will be always in this de Sitter solution. A small fluctuation away from H^* might derive the solution towards or away from

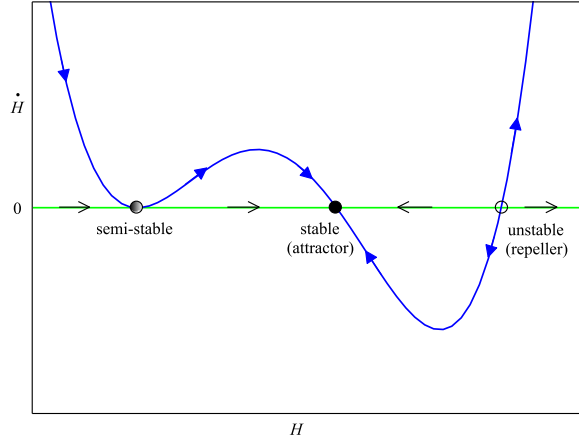


Figure 1. A toy-example of the phase space portrait that arises from (3.1) in $f(T)$ cosmology for notation clarification. The flow is towards the right when $\dot{H} > 0$ and towards the left when $\dot{H} < 0$. Moreover, the flow terminates at fixed points, which are the zero's of $\mathcal{F}(H)$ and are de Sitter solutions (3.1). The fixed points are classified to be unstable, stable or semi-stable according to the sign of their tangents. Unstable fixed points are represented by open circles with arrows emanating out of them, while stable points (attractors) are represented by closed circles with arrows pointing towards them. Finally, semi-stable points are represented by half-filled circles, and are stable from one side and unstable from the other side.

these points, depending on the type of the fixed point. Thus, the fixed points are classified to be *unstable*, *stable* or *semi-stable* according to the sign of their tangents. Unstable fixed points (repellers) are represented by open circles with arrows emanating out of them, as can be seen in the example Fig. 1. Stable points (attractors) are represented by closed circles with arrows pointing toward them. Finally, semi-stable are represented by half-filled circles, and are stable from one side and unstable from the other side.¹ In particular, differentiation with respect to time yields $\frac{d}{dt}(\delta H) = \frac{d}{dt}(H(t) - H^*) = \dot{H}$, since H^* is constant, and thus the perturbation in the Hubble space around H^* propagates with a rate

$$\frac{d}{dt}(\delta H) = \dot{H} = \mathcal{F}(H) = \mathcal{F}(H^* + \delta H). \quad (3.2)$$

Applying a Taylor expansion around the fixed point H^* as $\mathcal{F}(H^* + \delta H) = \mathcal{F}(H^*) + \delta H \mathcal{F}'(H^*) + O(\delta H^2)$, where $\mathcal{F}'(H^*) = \left. \frac{d}{dH} \mathcal{F}(H) \right|_{H^*}$ (we have used that $\mathcal{F}(H^*) = 0$ since H^* is a fixed point), we finally acquire $\frac{d}{dt}(\delta H) \approx \delta H \mathcal{F}'(H^*)$. Therefore, the linearization of δH around H^* leads to the solution

$$\delta H(t) \propto e^{\mathcal{F}'(H^*)t}.$$

The above equation shows that the slope $\mathcal{F}'(H^*)$ at the fixed point determines its stability. If $\mathcal{F}'(H^*) > 0$, all small disturbances $\delta H(t)$ grow exponentially and the fixed point in this case is unstable (repeller or source). If $\mathcal{F}'(H^*) < 0$, then all sufficiently small disturbances decay exponentially and the fixed point in this case is stable (attractor or sink). Finally, if the slope $\mathcal{F}'(H^*)$

¹This classification is closely related to the traditional way of linearizing the system $\dot{H} = \mathcal{F}(H)$ around a fixed point H^* , allowing for a small perturbation $\delta H(t) = H(t) - H^*$ around H^* , resulting to a differential equation for δH in order to check whether the perturbation decays or grows [105–111].

alters its sign at the fixed point (thus the fixed point is an extremum of $\mathcal{F}(H)$), it is a semi-stable phase point at which the solution is stable from one side and unstable from the other side. Lastly, in order to fix our notations we follow [124] and we call equation $\dot{H} = \mathcal{F}(H)$ the *phase portrait*, while its solution is the *phase trajectory*.

An important issue that needs to be mentioned is how fixed points (or singularities) in one-dimensional systems split solutions into different branches. In particular, one of the main features of a fixed point is that it can be reached only after infinite time, as long as \mathcal{F} is differentiable at that point (this can be easily seen by expanding \mathcal{F} around the fixed point and integrate $\dot{H} = \mathcal{F}(H)$ in order to acquire the time needed to reach that point), a condition that is satisfied in most models. An important consequence of this statement is that if a solution lies between two fixed points then it has to start from $t = -\infty$ at one point and reach the other fixed point at $t = +\infty$, which constitutes a solution branch by itself. In general, if a model has N fixed points, then we have $N + 1$ of the above regions and thus we obtain $N + 1$ different branches of solutions. Amongst others, and following [108], we can see that if $\mathcal{F}(H)$ is continuous and differentiable and there exists a future and a past fixed point, the solution is free from types I, II and III singularities classified in [125]. Additionally, in this case it is easy to show that there exists a no-go theorem stating that $H(t)$ cannot cross a fixed point, or $w_{eff} = -1$, at a finite time, since the time to reach this point is infinite.

Here we make a comment on the continuity and differentiability of $\mathcal{F}(H)$. Given an initial condition $H(t_0) = H_0$, the continuity of $\mathcal{F}(H)$ guarantees the existence of a solution, while its differentiability guarantees the uniqueness of the solution, see for example [124]. Nevertheless, from this important theorem one can deduce the limitations of the phase-space analysis, namely at the points where $\mathcal{F}(H) \rightarrow \infty$. In these cases there is no unique solution locally, and therefore it is not clear how the system will evolve in later times [124].

In summary, the above formalism provides a qualitative description of the behaviour of a cosmological scenario, without knowing any exact solution. In the following, we obtain the phase portraits of $f(T)$ cosmology in the $(\dot{H} - H)$ *phase space*, where each point is a *phase point* and could serve as an initial condition.

Let us now proceed in the application of the above dynamical-system method in the case of general $f(T)$ cosmology. As we mentioned, we can express the matter energy density and pressure as functions of H , that is using (2.18), (2.20), (2.21) and (2.22), we can write

$$\rho = \frac{1}{2\kappa^2} [\tilde{f}(H) - H\tilde{f}_H], \quad (3.3)$$

$$p = \frac{1}{6\kappa^2} \dot{H}\tilde{f}_{HH} - \rho, \quad (3.4)$$

where $\tilde{f}(H) = f(-6H^2)$, and $\tilde{f}_H := \frac{d\tilde{f}}{dH}$ and $\tilde{f}_{HH} := \frac{d^2\tilde{f}}{dH^2}$. Then, for a general barotropic matter fluid with $p = w\rho$, equations (3.3) and (3.4) give

$$\dot{H} = 3(1 + w) \left[\frac{\tilde{f}(H) - H\tilde{f}_H}{\tilde{f}_{HH}} \right] = \mathcal{F}(H). \quad (3.5)$$

Note that this equation is valid only if $\tilde{f}_{HH} \neq 0$. The case where $\tilde{f}_{HH} = 0$ at all times corresponds to $f(T) = \alpha\sqrt{-T} + \beta$, which is the known ‘‘trivial’’ $f(T)$ form for which the $f(T)$ effect is completely eliminated from the equations and the theory becomes trivial [21]. In this work we will not consider

this trivial case. However, one should pay attention to the fact that for a general $f(T)$ model, \tilde{f}_{HH} may become zero at a specific time, i.e $\mathcal{F}(H) \rightarrow \infty$. These points correspond to sudden singularities [125], and in order to fully analyze their properties one should propose a specific spacetime extension, which extend non-spacelike curves beyond these soft singularities as done in [108, 116, 126–129]. For completeness, note that the above method is fully applicable in the case where $f(T)$ gravity becomes TEGR, that is general relativity, i.e for $f(T) = T + \Lambda$, since in this case we always have $\tilde{f}_{HH} = -12 \neq 0$.

Equation (3.5) is the main equation of the one-dimensional autonomous system in general $f(T)$ cosmology. First of all, it determines the existence of fixed points and sudden singularities. In particular, the fixed points are obtained for $\tilde{f} = H \tilde{f}_H$ and they are reached after infinite time if $\mathcal{F}(H)$ is differentiable at this point. On the other hand, sudden singularities are points where \tilde{f}_{HH} vanishes. Points of sudden singularities are reached at finite time and it is generally possible to extend the spacetime beyond these points, as well as the curves of physical test particles, as has been shown in [116]. Note that these singularities are not related to the divergence of the energy density and/or pressure.

Finally, let us translate the basic observational constraints to a simple list of requirements about phase space diagrams which describe realistic cosmological models. In particular:

- (i) The late time acceleration might be modeled as flowing towards a future fixed point.
- (ii) The universe crossed from deceleration to acceleration at a redshift $z_{tr} \geq 0.6$ (the redshift is given by $z = \frac{a_0}{a} - 1$, where the current value of the scale factor a_0 is set to 1). According to (2.28) this “zero acceleration curve” corresponds to $q = 0$, i.e to $w_{eff} = -1/3$.
- (iii) The universe has passed from radiation and matter eras in the past.

3.2 Phase portraits of standard cosmological evolution

Let us now investigate the phase space portraits of $f(T)$ cosmology in which no singularities are involved, namely the universe behaves in the standard way. In order to incorporate more efficiently the three observational requirements described above, and in particular point (ii), we re-write (2.27) as

$$\dot{H} = -\frac{3}{2} (1 + w_{eff}) H^2. \quad (3.6)$$

Hence, one can study this equation in terms of the values of w_{eff} . In the following paragraphs we study the case of constant and varying w_{eff} separately.

3.2.1 Fixed effective equation of state

If w_{eff} is constant then (3.6) admits *only* the trivial solution $(\dot{H}, H) = (0, 0)$. Geometrically this null solution represents the origin of the phase space, which is also a Minkowskian fixed point. Thus, this null solution splits the phase space into two separate patches: In the first patch, corresponding to $H > 0$, the universe is expanding, while in the second patch, where $H < 0$, the universe is contracting. Notably, as we analyzed above, transitions between these two patches through the Minkowskian origin cannot be achieved in a finite time. In order to present the above features in a more transparent way, in Fig. 2 we construct the corresponding phase portrait, following the notation of the toy-example Fig. 1.

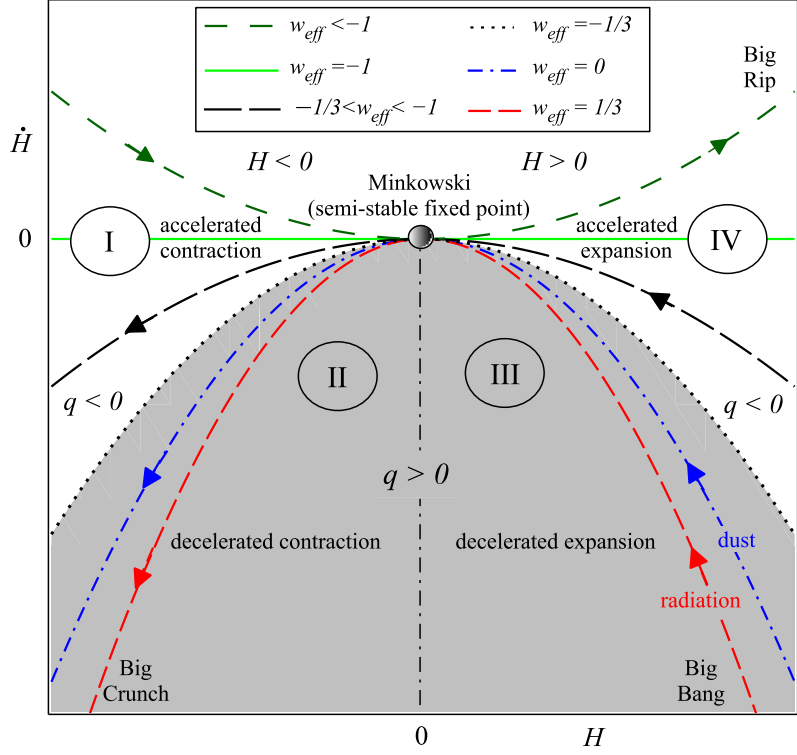


Figure 2. Phase space portraits according to (3.6), for various values of constant w_{eff} . The point at the origin corresponds to a semi-stable Minkowski universe. The dotted curve represents the zero acceleration boundary and it divides the phase space into two regions, namely the decelerated (shaded) and the accelerated (unshaded) region. The labels (I)-(IV) mark the regions with the four possible behaviours described in the text. The graph has scale invariance, and every shortening or extension which includes $(0, 0)$ will look the same.

The phase space, in general, contains four different dynamical regions according to the values of the Hubble function H and of the deceleration parameter $q \equiv -1 - \dot{H}/H^2$. Accordingly, we proceed to the following classification:

- (i) The unshaded region in the negative Hubble patch represents an accelerated contraction phase, since $H < 0$ and $q < 0$. We label this region as (I). The $dH/dt < 0$ region corresponds to $-1 < w_{eff} < -1/3$, while the $dH/dt > 0$ corresponds to $w_{eff} < -1$.
- (ii) The shaded region in the negative Hubble patch represents a decelerated contraction phase, since $H < 0$ and $q > 0$. We label this region as (II). In this region the universe evolves towards a future finite time singularity (Big Crunch).
- (iii) The shaded region in the positive Hubble patch represents a decelerated expansion phase, since $H > 0$ and $q > 0$. We label this region as (III). In this region the universe begins with a finite time singularity (Big Bang).
- (iv) The unshaded region in the positive Hubble patch represents an accelerated expansion phase,

since $H > 0$ and $q < 0$. We label this region as (IV). The $dH/dt < 0$ region corresponds to $-1 < w_{eff} < -1/3$ while the $dH/dt > 0$ corresponds to $w_{eff} < -1$.

Interestingly, we can unify two or more of these behaviours, obtaining a transition from expansion to contraction if we add a negative cosmological constant. In particular, the addition of a negative cosmological constant moves the phase portrait and the Minkowski fixed point towards the lower part of the figure, making the transition from expansion to contraction realizable. On the other hand, under the addition of a positive cosmological constant the phase portrait will be shifted vertically towards the upper part of the figure, and thus the Minkowskian fixed point will be moved upwards providing two new fixed points, which will allow for the transition from contraction to expansion, that is for the bounce realization [117].

In the rest of the manuscript we will follow the color notation of Fig. 2, corresponding to the above four regions. Finally, we mention here that in the case of a fixed w_{eff} , the one-dimensional autonomous systems do not allow for oscillating solutions, since crossing the phantom divide line $w_{eff} = -1$ requires an infinite time.

3.2.2 Dynamical effective equation of state

In a general and more realistic case of $f(T)$ cosmology w_{eff} is not constant, but it is a function of H , as was described in detail in the beginning of this section. In this case, one must fulfill the basic observational requirements listed above. In Fig. 3 we present schematic phase space portraits of some generic and realistic cosmological models, which can in principle arise within the framework of the $f(T)$ cosmology. Let us analyze some of their features, examining for simplicity separately the regimes that have different Hubble function values.

- Large Hubble function regime.

Imposing the known observational constraints, we list all possible $f(T)$ cosmologies according to their behaviour at large H . In order to obtain an early accelerated expansion epoch (inflation), the phase portrait at large H should lie within region IV. This constraint leads us to distinguish between three different scenarios depending on the behaviour of \dot{H} at early times:

$$t = \int_{H>0}^{H^*} \dot{H}^{-1} dH = \begin{cases} \infty, & H^* = \text{finite}, \dot{H} = 0 \text{ (scenario A)}; \\ \infty, & H^* \rightarrow \infty, \dot{H} \rightarrow \infty \text{ (scenario B)}; \\ \text{finite}, & H^* \rightarrow \infty, \dot{H} \rightarrow \infty \text{ (scenario C)}. \end{cases} \quad (3.7)$$

In scenario A, as shown in Fig. 3, the phase portrait begins with a fixed point in the past, i.e. $\dot{H} = 0$, with a very large value of H (close to the Planck value, $H^* = H_{Planck} = 1/l_{Planck}$). Eq. (3.7) implies that the time required to reach this point is infinite, which enables a non-singular description of the universe evolution and can in principle describe inflation. In scenario B, the phase portrait asymptotically exhibits a linear (or slower) behaviour. The phase portrait in this case is characterized by $\dot{H} \propto H^s$, where $s \leq 1$ as $H \rightarrow \infty$, and then the integral in (3.7) diverges. In this scenario the universe has a Big Bang singularity, however it is pushed back to infinite time. In scenario C, the universe begins with a Big Bang singularity with an asymptotic effective equation-of-state parameter $-1 < w_{eff} < -1/3$ for large H . The phase portrait in this case is characterized by $\dot{H} \propto H^s$, where $s > 1$ as $H \rightarrow \infty$, and then

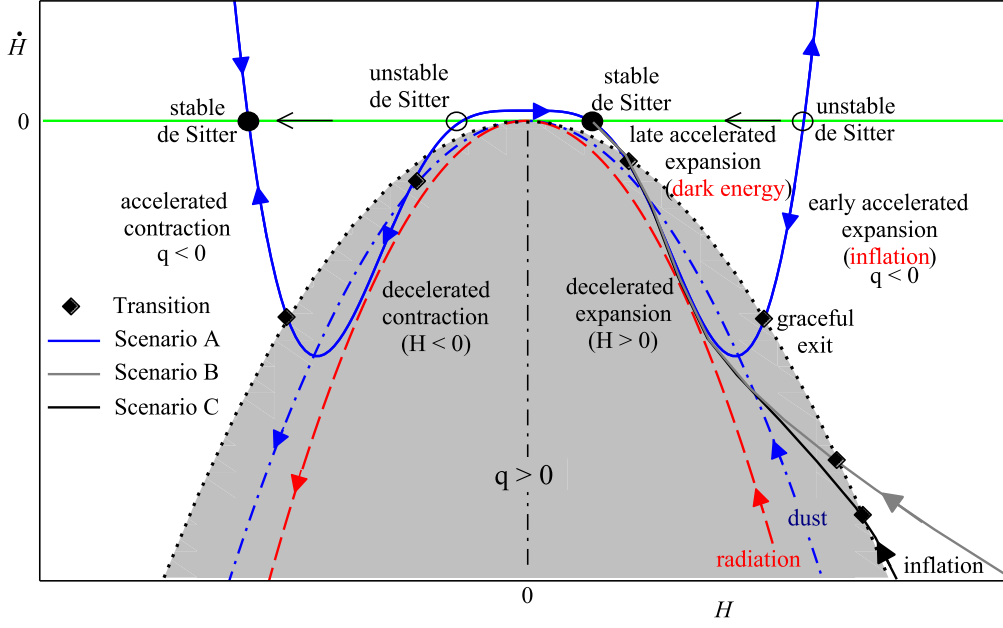


Figure 3. Phase space portraits according to (3.6), in the general case where $w_{eff} \equiv w_{eff}(H)$. The three scenarios, the transition points, and the behaviour at different Hubble regimes are described in the text. The dust and radiation curves are the same with Fig. 2 and are drawn for convenience. The scale of the graph is determined by the unstable de Sitter point at $H^* = H_{Planck} = 1/l_{Planck}$.

the integral in (3.7) is finite. In these three different scenarios, the phase portraits should intersect the zero acceleration curve into the radiation curve at region (III) where Hubble function acquires smaller values. At the intersection point $\dot{H} = -H^2$, the universe terminates its accelerated expansion phase. Therefore, the universe can exit into the FRW decelerated expansion, and thus the Hubble parameter should be chosen $H \sim 10^7$ GeV in order to obtain a graceful exit.

- Intermediate Hubble function regime.

This regime characterizes the standard cosmological era, and the $f(T)$ models can give rise to a successful thermal history just as predicted by standard cosmology. Hence, the phase portraits of scenarios A - C of Fig. 3 in this regime correspond to the radiation era.

- Small Hubble function regime.

The phase portraits intersect the zero acceleration curve, namely $\dot{H} = -H^2$, for the second time, allowing the universe to transform into a late-time accelerated expansion phase. This point imposes a further constraint, since as we mentioned above, the late-time transition to acceleration is expected to be at redshift $z_{tr} \gtrsim 0.6$, i.e at $H_{tr} \gtrsim 100$ km/s/Mpc. Additionally, in this regime the three scenarios A - C exhibit a similar behaviour.

- Fate of the universe.

In the future, when H^2 becomes comparable to the cosmological constant, the phase portrait evolves towards a future de Sitter fixed point with $w_{eff} \sim -1$, as can be seen in Fig. 3. However, in some cases the universe may evolve towards Minkowski instead of de Sitter (we did not include this case in Fig. 3 since it is in tension with Λ CDM paradigm).

We close this paragraph by mentioning that in order to draw Fig. 3 we did not use explicit $f(T)$ forms, since our purpose is to show how the Hubble-rate flow in phase space is constrained by basic observational requirements, and moreover how these constraints allow for three qualitatively different scenarios at large \dot{H} . Nevertheless, by considering an explicit form of $\dot{H} \equiv \mathcal{F}(H)$, which reproduces any of the scenarios given in Fig. 3, the corresponding $f(T)$ gravity can be obtained from Eq. (3.5). On the other hand, the observational requirements obtained from crossing the zero acceleration curve, either at large or small Hubble function regimes, can be used as usual to determine the free parameters of the $f(T)$ theory.

3.3 Phase portraits of finite-time singularities of Type II and IV

In the previous subsection we investigated the phase space portraits of $f(T)$ cosmology, focusing on the standard cosmological evolution, namely in the absence of singularities. Hence, the only singularities that might possibly appear were those characterized by $\dot{H} \rightarrow \pm\infty$ as $H \rightarrow \pm\infty$, namely the asymptotic behaviour of the parabolic phase portrait, which correspond to the finite-time singularities of Type III of [125], such as the Big Bang and Big Crunch. In the present subsection we wish to extend our investigation of the phase space portraits in order to explore more exotic cosmological evolutions such as the phantom-divide crossing, the bounce realization, the Big Brake and the cosmological turnaround. Such evolutions may incorporate the appearance of soft finite-time singularities of type II and IV [108, 117, 125]. As it is known, such exotic cosmological behaviours are impossible in the framework of general relativity, since in this case the various energy conditions violations that are necessary for their realization cannot be obtained [130, 131]. However, it is also known that they are possible in the framework of modified gravity. We mention that at the observational level, neither Type II nor IV represent harmful singularities [125]. In the following, examining the phase space portraits, we show that they can be realized in the framework of $f(T)$ cosmology.

3.3.1 Non-singular bounce

In Fig. 4 we present a schematic phase space portrait of a non-singular bounce [132, 133]. In such a phase portrait the flow is clockwise, and the system passes by the four regions of the phase space. This pattern has been studied in detail in [117]. The universe in this scenario has an (eternal in the past) Minkowskian fixed-point origin, and then it enters into region (II), that is into a decelerated contraction phase. The phase portrait then intersects the zero curve acceleration and the universe enters into an accelerated contraction, namely into region (I), where $\dot{H}_- < 0$. However, the phase portrait crosses the phantom divide line $\dot{H} = 0$, entering into an effectively phantom phase where $\dot{H}_+ > 0$.

Although crossing the phantom divide line is realized through a de Sitter fixed point, the time needed to reach it is not infinite. In order for this exceptional case to be realized, the following conditions at the fixed point must be fulfilled [108]:

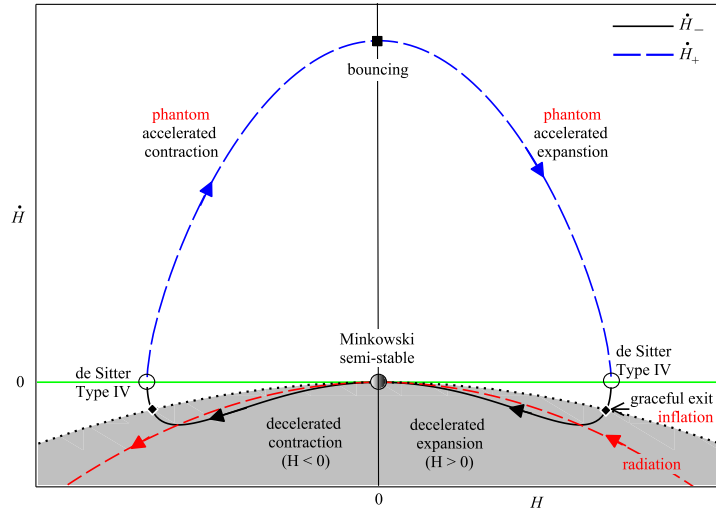


Figure 4. Schematic phase space portrait for non-singular bounce realization. The blue-dashed curve corresponds to $\dot{H}_+ > 0$, while the black-solid to $\dot{H}_- < 0$. Similarly to the previous figures, the black-dotted and the red-dashed curves are respectively the zero acceleration boundary and the radiation curve, and are drawn for convenience. The scale of the graph is determined by the Type IV de Sitter singular point at $H = H_f$.

- (i) $\dot{H}|_{H=H_f} = 0$,
- (ii) $d\dot{H}/dH|_{H=H_f}$ diverges,
- (iii) $t = \int_H^{H_f} \dot{H}^{-1} dH = \text{finite}$,
- (iv) the phase portrait is double-valued around the fixed point H_f .

The first three conditions are required in order for the fixed point to be reached in a finite time, while the fourth one is necessary for the crossing. It is not difficult to show that the fixed point in this case is in fact a Type IV singular point according to the finite time singularity classification [125], where all the quantities a , H and \dot{H} are finite but the second derivative $\ddot{H} = \dot{H} \left(\frac{d\dot{H}}{dH} \right)$ diverges at $H = H_f$. Therefore, we call this type of fixed points a Type IV de Sitter point. On the phase portrait such points can be recognized, since on them the portrait has an infinite slope.

In the phantom phase, in the $\dot{H}_+ > 0$ branch, the universe transits from region (III), which is a phase of accelerated contraction ($H < 0$), into region (IV), which is a phase of accelerated expansion ($H > 0$), and throughout this procedure we have $\dot{H} > 0$. Thus, the bouncing point² is the point ($H = 0$, $\dot{H} > 0$). In the end of the phantom phase, the universe crosses the phantom divide line through a Type IV de Sitter point, as indicated by the phase portrait of Fig. 4.

²At the bounce point the comoving Hubble horizon $R_H = \frac{1}{aH}$ is infinite as H is null, and thus all comoving modes k are subhorizon. After the bounce, R_H shrinks to a minimal value and therefore some modes are allowed to exit the horizon and transform to classical modes. Additionally, the scale invariant power spectrum can be obtained just as in inflationary scenario. Nevertheless, in non-singular bounce the trans-Planckian problems of inflation can be avoided [132].

Finally, note that the phase portrait intersects the zero acceleration curve smoothly, entering into the FRW decelerated expansion phase, i.e region (III). During this era the phase portrait matches standard cosmology, and thus it leads to the usual thermal history. However, the universe evolves towards the Minkowskian origin without exhibiting the late-time acceleration phase.

3.3.2 Singular bounce

In Fig. 5 we present an example of a phase portrait that can smoothly cross the phantom divide line $\dot{H} = 0$ just as in non-singular bounce. However, $\dot{H} > 0$ diverges at $H = 0$ producing a Type II “sudden” finite-time singularity associated with the bouncing point. The interesting feature is that in this case the scale factor and its first derivative at this singularity type are finite, and consequently the Christoffel symbols are finite too. In case of sudden singularities in the framework of general relativity it has been shown that physical geodesics are in principle extendible [134–136]. In subsequent works some specific extensions have been proposed, in addition of applying suitable junction conditions at $H = 0$ to ensure consistency between the geodesic extensions and the field equations [128, 129]. In the case of singular bounces the comoving Hubble radius R_H is finite at the bounce point and not all the comoving modes are subhorizon. Hence, such models are phenomenologically different from the non-singular bounce [132].

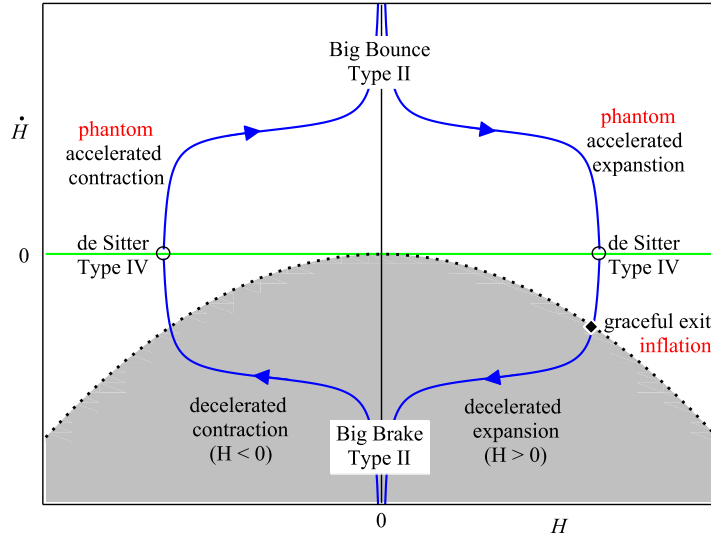


Figure 5. Schematic phase space portrait for singular bounce realization, in which the bounce happens through a Type II (sudden) singularity. Similarly to the previous figures, the black-dotted curve marks the zero acceleration boundary. The scale of the graph is determined by the Type IV de Sitter singular point at $H = H_f$.

On the other hand, if $\dot{H} < 0$ diverges at $H = 0$ then the phase portrait exhibits the Big Brake cosmology. The general relativistic version of this model suffers from the so-called “soft singularity crossing paradox” [128, 137, 138], where the matter density does not vanish at the braking point. However, as we can now see, instead of adding exotic matter such as anti-Chaplygin gas or tachyon fields to overcome this problem, one can use $f(T)$ gravity. The reconstruction of the $f(T)$ gravity

which generates phase portraits corresponding to the Big Brake realization was given in [118]. Furthermore, the junction condition in $f(T)$ gravity has been applied in Big Brake scenario in [116]. Finally, as we observe from Fig. 5, if the phase portrait has a cusp at $H = 0$ with finite value of \dot{H} , then the bounce/Big Brake point is associated with a finite-time singularity of Type IV.

In summary, in order for a phase portrait to cross the phantom divide line smoothly it must be through a de Sitter fixed point of Type IV. However, in order for a phase portrait to cross between contraction and expansion in singular cosmology, it must be through a finite time singularity of Type II or IV.

4 Cosmological phase portraits of specific $f(T)$ models

In the previous section we investigated the phase space portraits of general $f(T)$ cosmology, and we extracted the general features and behaviours without specifying to individual models. In the present section we apply the general method to the specific viable models that have been studied in the literature. As we can see, we can extract the results already obtained in the literature using the standard dynamical system methods [112–114], and moreover we can provide additional information concerning the global behaviour of the universe, focusing on their differences and similarities.

In particular, in the following three subsections we will separately study the power-law, the square-root exponential, and the exponential $f(T)$ models. These three models are the viable ones, since they are in the best agreement with cosmological observations and Solar System constraints [51, 76–78, 139, 140], and they are characterized by two parameters, one of which is independent.

4.1 f_1 CDM model: $f(T) = T + \alpha(-T)^b$

The power-law $f(T)$ model (hereafter f_1 CDM model) reads as [121]

$$f(T) = T + \alpha(-T)^b, \quad (4.1)$$

with α and b the two model parameters (the former is dimensionful with units of $[\text{length}]^{2(b-1)}$, while the later is dimensionless). Inserting (4.1) into (2.20) and then into the first Friedmann equation (2.18) at current time we obtain the relation between α and b , namely

$$\alpha = (6H_0^2)^{1-b} \frac{1 - \Omega_{m,0}}{2b - 1}, \quad (4.2)$$

where $\Omega_{m,0} = \frac{\kappa^2 \rho_0}{3H_0^2}$ is the current value of the matter density parameter, namely at scale factor $a_0 = 1$ (the subscript “0” marks the current value of a quantity). In the case $b = 0$ the model at hand coincides with TEGR, i.e general relativity, with a cosmological constant, that is to Λ CDM cosmology.

Inserting (4.1) into (3.5) we acquire

$$\dot{H} = -\frac{3}{2}(1+w)H^2 \left[\frac{1 - \alpha(2b-1)(6H^2)^{b-1}}{1 - \alpha b(2b-1)(6H^2)^{b-1}} \right]. \quad (4.3)$$

Since we are interested in the dark energy era, we focus on the case of dust matter and we use $w = 0$. Additionally, we impose $\Omega_{m,0} = 0.318$ and $H_0 = 76.11$ km/s/Mpc in agreement with observations [141].

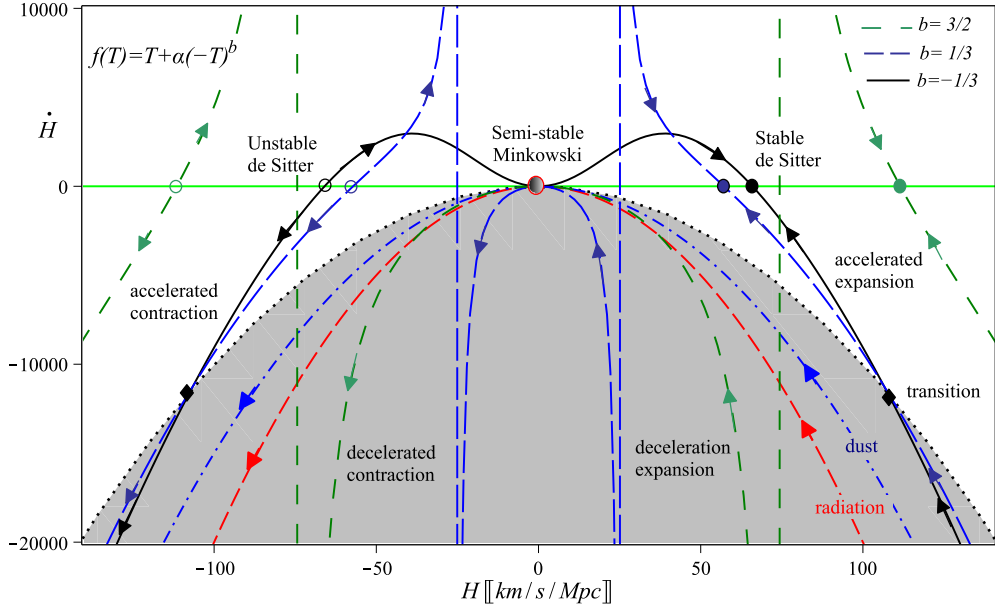


Figure 6. Phase space portraits for the power-law f_1 CDM model of (4.1), according to (4.3), for three values of the model parameter b . Similarly to the previous figures, the zero acceleration boundary and the dust and radiation curves, are drawn for convenience. The scale of the graph is determined by the value of $T_0 = -6H_0^2$, and thus by the imposition of $H_0 = 76.11$ km/s/Mpc.

In Fig. 6 we present the phase space portraits of the power-law $f(T)$ model (4.1), for three choices of the parameter b . In the $H > 0$ half-plane we identify the fixed points by setting $\dot{H} = 0$ in (4.3), and in the examples of the figure they correspond to $H^* = 65.95$, 57.15 and 111.51 km/s/Mpc for $b = -1/3$, $1/3$ and $3/2$, respectively. These points represent stable de Sitter future attractors, and the time required to approach them is infinite since \dot{H} is finite. We are interested in the $(H > H^*)$ -patch, where the transition from decelerated to accelerated expansion is realized. The phase trajectory in this region goes towards the left, i.e towards the decreasing H direction. The phase portrait shows that the universe begins with an initial singularity (Big Bang), it exhibits a matter-dominated era, and then it enters into the late-time acceleration phase. The realization of this epoch sequence favors $b = -1/3$, $1/3$, in which the acceleration transition occurs at $H_{tr} = 107.36$ km/s/Mpc (for $b = -1/3$) and at $H_{tr} = 107.89$ km/s/Mpc (for $b = 1/3$), i.e at redshift $z_{tr} \sim 0.6$ (for a discussion on the transition redshift in various $f(T)$ cosmological models see [75]). Moreover, the model parameter b can be constrained by knowing the transition time more precisely. This can be done by determining the intersection of the phase portrait with the zero acceleration curve by setting $\dot{H} = -H^2$ at $H = H_{tr}$. Using (4.3) we find

$$\alpha = -\frac{(6H_{tr}^2)^{1-b}}{(2b-1)(2b-3)}, \quad (4.4)$$

and comparing with (4.2) we extract the useful relation

$$H_{tr} = \frac{H_0}{(2b-3)^{\frac{1}{2(b-1)}}(\Omega_{m,0}-1)^{\frac{1}{2(b-1)}}}, \quad (4.5)$$

which predicts the Hubble parameter value at the transition as a function of b . Some specific values are presented in Table 1. It is worth mentioning that relation (4.5) restricts the parameter b to be less than $3/2$ if we impose the physical requirement $\Omega_{m,0} < 1$.

b	H_{tr} [km/s/Mpc]	z_r
0	~ 108.91	~ 0.61
0.05 or 0.17	~ 109.01	~ 0.63
0.07 or 0.15	~ 109.04	~ 0.63
-0.36 or 0.38	~ 107.18	~ 0.60
-0.92 or 0.5	~ 103.92	~ 0.55

Table 1. Values of the Hubble parameter and of the redshift at the transition, for the power-law f_1 CDM model of (4.1), according to (4.5), for various values of the model parameter b .

In order to cover all possible scenarios we discuss the case where $b = -1/3$ and the initial Hubble value $0 < H_i < H^*$. From Fig. 6 we observe that the universe interpolates smoothly between semi-stable Minkowski and stable de Sitter at $-\infty \leq t \leq \infty$. Thus, the universe is non-singular and evolves effectively in a phantom-like regime as $\dot{H} > 0$. In addition, we can also see two other possible behaviours in contraction phases ($H < 0$), where $-H^* < H_i < 0$ and $H_i < H^*$.

We close the analysis of this model by examining the fulfillment of basic observational requirements. As we mentioned above, the power-law $f(T)$ model (4.1) reduces to Λ CDM cosmology for $b = 0$, and thus we expect that the favored b -values of the model will be around this value. Indeed, confrontation with observations yields that the best fit on the parameter b , as measured from the combined cosmic chronometers (CC) + H_0 + Supernovae Type I (SNIa) + Baryon Acoustic Oscillations (BAO) observational data, is $b = 0.05536$ [76]. Then, the parameter α from (4.2) is found to be $\alpha \sim -1.0543 \times 10^{-43} \text{ km}^{-1.8893}$ (the units of α are $\text{km}^{-2(1-b)}$). These values are confirmed by different data sets too, and in general at 3σ one obtains $-1/3 \leq b \leq 1/3$ [77, 78, 139].

Finally, apart from the correct behaviour at late times we need to ensure that the model can realize the matter era too, and it proves that the phase portrait analysis can be a powerful tool for this goal. In particular, examining the asymptotic behaviour of phase portrait (4.3) at early times, namely at $H \gg H_{tr}$, for $b \leq 1$ we find that $\dot{H} = -\frac{3}{2}(1+w)H^2$, while for $b > 1$ we obtain $\dot{H} = -\frac{3}{2}\frac{(1+w)}{b}H^2$, where the equation of state has to be set to $w = 0$ since we focus on the dust case. Therefore, it is obvious that the matter dominated era can be obtained only in the regime $b \leq 1$, which is consistent with the constraint of obtaining late-time acceleration.

In summary, as we see from the application of the phase space portraits, the power-law $f(T)$ model can lead to interesting phenomenology.

4.2 f_2 CDM model: $f(T) = T + \alpha T_0 \left(1 - e^{-p\sqrt{T/T_0}}\right)$

In this model the $f(T)$ has a square-root exponential form [122]

$$f(T) = T + \alpha T_0 \left(1 - e^{-p\sqrt{T/T_0}}\right), \quad (4.6)$$

where α and p are the two model parameters. Inserting (4.6) into (2.20) and then into the first Friedmann equation (2.18) at current time we acquire

$$\alpha = \frac{1 - \Omega_{m,0}}{1 - (1+p)e^{-p}}. \quad (4.7)$$

This model reduces to Λ CDM cosmology for $p \rightarrow +\infty$. Inserting (4.6) into the $f(T)$ phase portrait (3.5) we obtain

$$\dot{H} = -\frac{3}{2}(1+w)H^2 \left\{ \frac{1 - \alpha \left(\frac{H_0}{H}\right)^2 \left[1 - (1+pH/H_0)e^{-pH/H_0}\right]}{1 - \frac{1}{2}\alpha p^2 e^{-pH/H_0}} \right\}. \quad (4.8)$$

Focusing on the dust matter case $w = 0$, in Fig. 7 we present the phase space portrait of the square-root exponential model (4.6) for some choices of the parameter p . The fixed points correspond to $H^* = 137.10, 56.89$ and -12.69 km/s/Mpc, for $p = -2/3, 3$ and $1/2$, respectively. As we observe, the phase portrait for $p = 1/2$ reproduces the standard cosmology in $H > 0$ region, however it does not possess a Minkowskian fate. Since its fixed point is $H^* < 0$, the universe will result into a contracting phase at asymptotically late times, i.e the cosmological turnaround will be realized. On the other hand, the phase portrait for $p = 3$ leads to a universe evolution in agreement with standard cosmology one. Moreover, the deceleration-to-acceleration transition occurs at $H = 112.78$ km/s/Mpc, namely at $z \sim 0.68$, in agreement with observations [141].

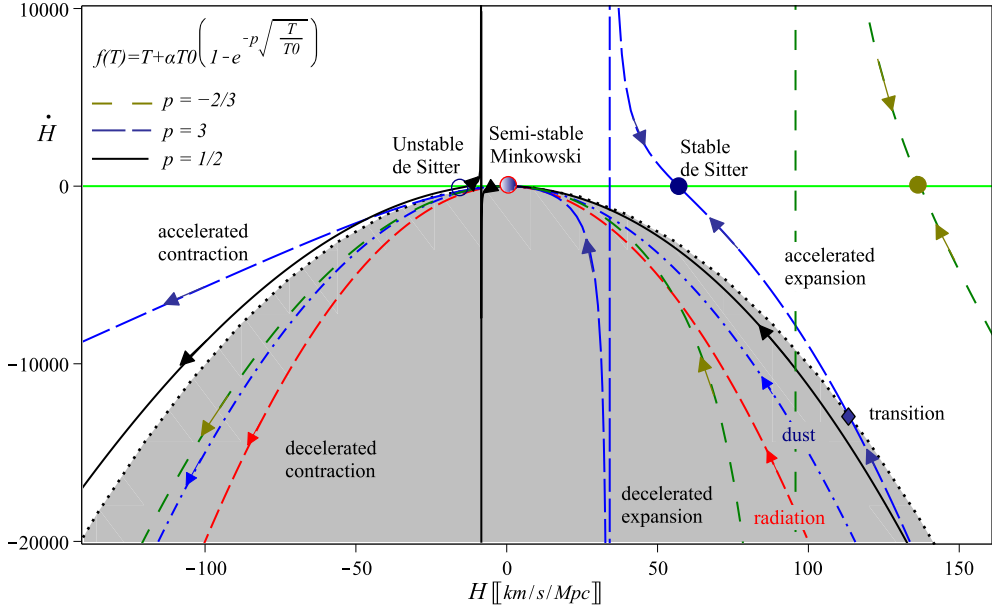


Figure 7. Phase space portraits for the square-root exponential f_2 CDM model of (4.6), according to (4.8), for three values of the model parameter p . Similarly to the previous figures, the zero acceleration boundary and the dust and radiation curves, are drawn for convenience. The scale of the graph is determined by the value of $T_0 = -6H_0^2$, and thus by the imposition of $H_0 = 76.11$ km/s/Mpc.

Let us now examine for which values of the parameter p the model is closer to the observed evolution. Concerning late times we saw that the larger the p is, the better is the behaviour. Ex-

amining the asymptotic behaviour of phase portrait (4.8) at early times, namely at $H \gg H_{tr}$, for $p < 0$ we find that $\dot{H} = \frac{3(1+w)}{p}H_0H$, while for $p > 0$ we obtain $\dot{H} = -\frac{3}{2}(1+w)H^2$, where w has to be set to 0 since we focus on the dust case. Therefore, for $p < 0$ the phase portrait does not accept the correct matter era (nevertheless, as can be seen from Fig. 7, the phase portrait grows linearly as $H \rightarrow \infty$ and thus it has no initial finite-time singularity, since it can be shown that if $\dot{H} \propto H^r$ ($r \leq 1$) asymptotically then the initial singularity is absent [108]). On the other hand, for $p > 0$ we obtain the correct matter era. These intervals are in agreement with the fact that Λ CDM cosmology is obtained for $p \rightarrow +\infty$. In particular, the combined CC + H_0 + SNIa + BAO observational data yield a best-fit value $b = 0.04095$, for $b = 1/p$ [76] and consequently, via (4.7), we obtain for the dimensionless parameter $\alpha = 0.7302$. Additionally, these values are confirmed by different data sets too, and in general at 3σ one obtains $p \geq 3$ [77, 78, 139].

We close the analysis by mentioning that as can be observed from Figs. 6 and 7, f_1 CDM and f_2 CDM models exhibit common features in the $H > 0$ patch, if we make the interchange $p = -1/b$ for $p < 0$, or $p = 1/b$ for $0 < p < 1$. However, in the contraction patch $H < 0$ they present different behaviours.

4.3 f_3 CDM model: $f(T) = T + \alpha T_0(1 - e^{-pT/T_0})$

In this model the $f(T)$ has an exponential form [142]

$$f(T) = T + \alpha T_0(1 - e^{-pT/T_0}), \quad (4.9)$$

where α and p are the two model parameters. Inserting (4.9) into (2.20) and then into the first Friedmann equation (2.18) at current time we acquire

$$\alpha = \frac{1 - \Omega_{m,0}}{1 - (1 + 2p)e^{-p}}. \quad (4.10)$$

This model reduces to Λ CDM cosmology for $p \rightarrow +\infty$. Inserting (4.9) into the $f(T)$ phase portrait (3.5) we obtain

$$\dot{H} = -3(1+w)H_0^2 \left\{ \frac{H^2 - \alpha \left[H_0^2 - (H_0^2 + 2pH^2)e^{-\frac{pH^2}{H_0^2}} \right]}{2H_0^2 + 2\alpha p(H_0^2 - pH^2)e^{-\frac{pH^2}{H_0^2}}} \right\}. \quad (4.11)$$

In Fig. 8 we present the phase space portrait of the exponential model (4.9) for some choices of the parameter p , for the case of dust matter $w = 0$. The fixed points are obtained for $H^* = \pm 92.22$, 0 and ± 58.34 km/s/Mpc, for $p = -2/3$, 3 and $1/2$, respectively. As we can see, the choice $p = -2/3$ cannot lead to a universe evolution in agreement with the observed one. For $p = 1/2$ and $p = 3$ we can see that the deceleration-to-acceleration transition occurs at $H = 134.93$ and 134.14 km/s/Mpc respectively. However, for $p = 3$ the phase portrait indicates another transition back to deceleration at $H \sim 84.1$ km/s/Mpc, with a finite time singularity, while for $p = 1/2$ the universe can evolve towards a future fixed point. In general, the larger the value of p is, the more realistic is the cosmological behavior. This is in agreement with the fact that Λ CDM cosmology is obtained for $p \rightarrow +\infty$. Moreover, this is confirmed by detailed confrontation with observations, using combined

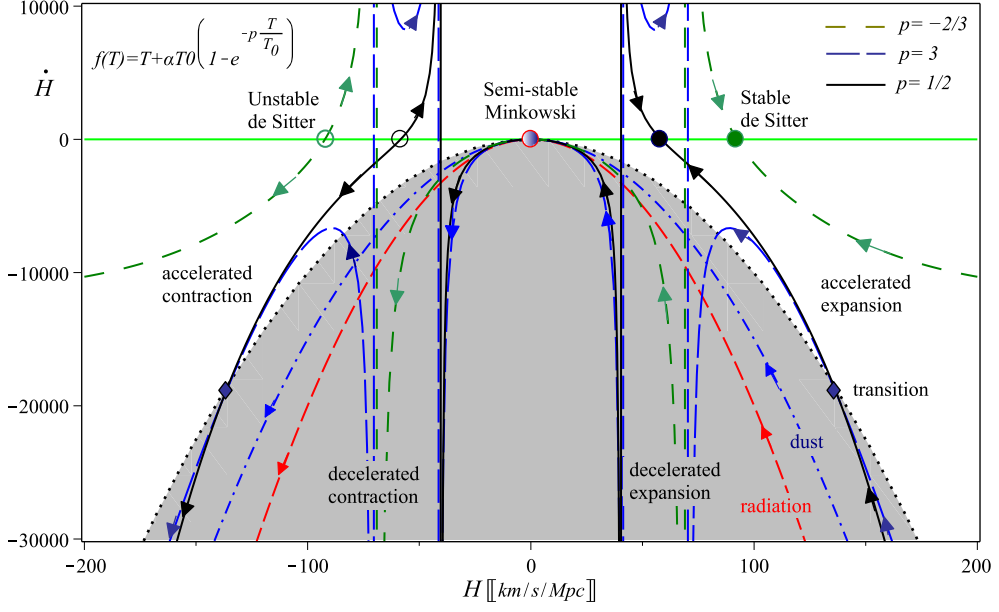


Figure 8. Phase space portraits for the exponential $f_3\text{CDM}$ model of (4.9), according to (4.11), for three values of the model parameter p . Similarly to the previous figures, the zero acceleration boundary and the dust and radiation curves, are drawn for convenience. The scale of the graph is determined by the value of $T_0 = -6H_0^2$, and thus by the imposition of $H_0 = 76.11 \text{ km/s/Mpc}$.

CC + H_0 + SNIa + BAO data sets, which yield a best-fit value $b = 0.03207$ for $b = 1/p$, and consequently, through (4.10) to $\alpha = 0.7352$ [76]. In general, at 3σ one obtains $p \geq 3$ [76–78, 139].

Finally, examining the asymptotic behaviour of the phase portrait (4.11) at early times, namely at $H \gg H_{tr}$, for $p < 0$ we find that $\dot{H} = \frac{3}{2} \frac{(1+w)}{p} H_0^2$, while for $p > 0$ we obtain $\dot{H} = -\frac{3}{2}(1+w)H^2$, where the equation of state has to be set to $w = 0$ since we focus on the dust case. Hence, in the parameter region $p < 0$ the phase portrait asymptotically evolves towards a constant value and thus the model does not accept the correct matter era. On the other hand, for $p > 0$, apart from late-time acceleration, the model exhibits the correct matter epoch at early times.

5 A new viable $f(T)$ model

In the previous section we used the basic advantage that in $f(T)$ cosmology in a flat FRW geometry all quantities can be expressed as functions of the Hubble function H , and we transformed the cosmological equation into a one-dimensional autonomous system whose phase space portraits could reveal the basic cosmological features and behaviours. Additionally, after we explored the general properties of $f(T)$ cosmology, we studied three specific viable $f(T)$ models characterized by two parameters, which are in the best agreement with observations. In the present section we use as a guide the basic features arisen from the above investigation of the phase space portraits, in order to construct a new model of $f(T)$ gravity. This model proves to be efficient in the description of the cosmological history of the universe.

5.1 The model: $f(T) = T e^{\beta T_0/T}$

The simple model that we propose in this work is

$$f(T) = T e^{\beta T_0/T}, \quad (5.1)$$

where β is the single dimensionless model parameter. Inserting this relation into (2.20), (2.21), and using (2.17), namely that $T = -6H^2$, we find

$$\rho_T(H) = \frac{3}{\kappa^2} \left[H^2 - (H^2 - 2\beta H_0^2) e^{\beta \frac{H_0^2}{H^2}} \right], \quad (5.2)$$

$$p_T(H) = -\frac{3\beta H_0^2 H^2}{\kappa^2} \left[\frac{H^2 + 2\beta H_0^2}{H^4 - \beta H_0^2 H^2 + 2\beta^2 H_0^4} \right], \quad (5.3)$$

and thus the (torsion originated) dark energy equation-of-state parameter becomes

$$w_T(H) = \frac{-\beta H_0^2 H^2 (H^2 + 2\beta H_0^2)}{\left[H^4 - \beta H_0^2 H^2 + 2\beta^2 H_0^4 \right] \left[H^2 - (H^2 - 2\beta H_0^2) e^{\beta \frac{H_0^2}{H^2}} \right]}. \quad (5.4)$$

Inserting (5.2) into the first Friedmann equation (2.18) at current time we express β in terms of the current value of the matter density parameter, namely

$$\beta = \frac{1}{2} + W \left(-\frac{1}{2} e^{-1/2} \Omega_{m,0} \right), \quad (5.5)$$

where $W(x)$ denotes the Lambert- W function, which is the solution of the transcendental equation $W e^W = x$. Using $\Omega_{m,0} = 0.318$, we acquire $\beta \sim 0.393$, or $\beta \sim -3.127$.

5.2 Phase space portraits

Let us now explore the phase space portrait of the new $f(T)$ model (5.1). Inserting (5.2) and (5.3) into the conservation equation (2.22) (or inserting it straightaway into (3.5)) we obtain the one-dimensional phase-portrait equation

$$\dot{H} = -\frac{3}{2}(1+w) \frac{(H^2 - 2\beta H_0^2) H^4}{H^4 - \beta H_0^2 H^2 + 2\beta^2 H_0^4}. \quad (5.6)$$

In Fig. 9 we present the corresponding phase portrait for the two values of β calculated above, corresponding to $\Omega_{m,0} = 0.318$ through (5.5). Note that for $\beta < 0$ the system has exactly one fixed point at $H = 0$, while for $\beta > 0$ there exist three fixed points at $H = 0, \pm \sqrt{2\beta} |H_0|$. Nevertheless, both β cases exhibit a transition from deceleration to acceleration at late times. Additionally, at early times, namely at large H , both β cases can describe the correct matter era, since in this regime we asymptotically have $\dot{H} = -\frac{3}{2}(1+w)H^2$.

Let us now discuss in more details the phase-space portrait features for the two β cases separately.

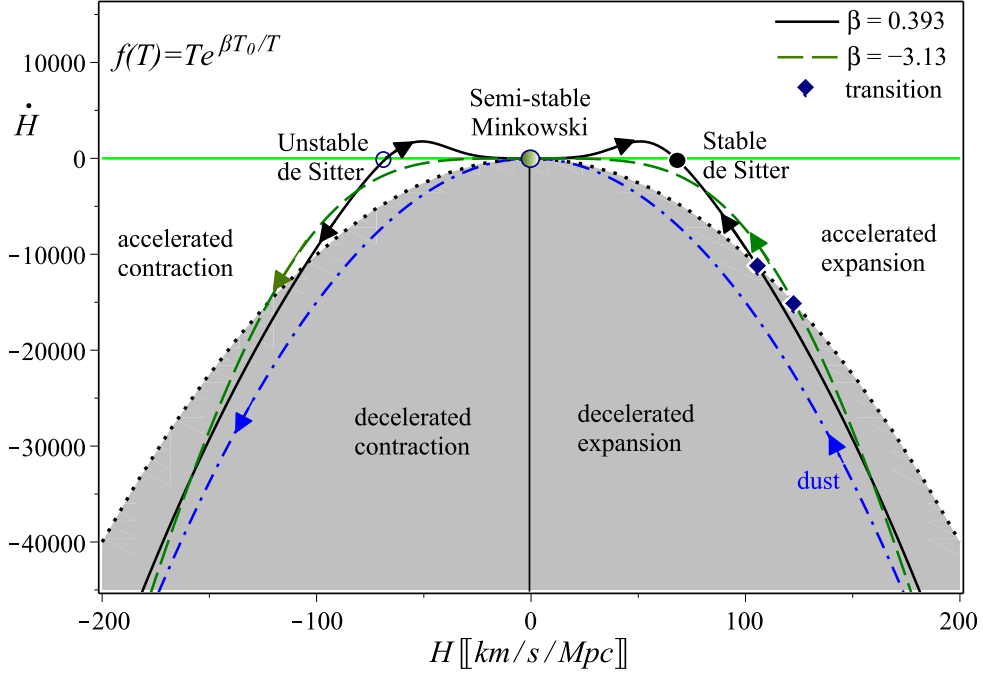


Figure 9. Phase space portraits for the new model of (5.1), according to (5.6), for two values of the model parameter β . Similarly to the previous figures, the zero acceleration boundary and the dust curve are drawn for convenience. The scale of the graph is determined by the value of T_0 , and thus by the imposition of $H_0 = 76.11 \text{ km/s/Mpc}$.

- $\beta < 0$. As we observe from Fig. 9, the phase portrait splits the phase space into two patches: (i) When $H < 0$ the universe has no initial singularity but it contracts towards a future Big Crunch, namely towards a finite-time singularity. (ii) When $H > 0$, the universe begins with a Big Bang singularity, it matches standard cosmology during the intermediate-time region, and it exhibits a late-time acceleration phase. However, unlike Λ CDM model, the universe evolves towards a Minkowskian future fixed point.
- $\beta > 0$. As we can see from Fig. 9, the phase portrait splits the phase space into four distinguishable patches: (i) When $H < -\sqrt{2\beta} |H_0|$ the universe does not have a past singularity, it is contracting, and it evolves towards a future Big Crunch singularity. (ii) When $-\sqrt{2\beta} |H_0| < H < 0$, the universe is contracting and non-singular, interpolating smoothly between de Sitter and Minkowski solutions in a phantom-like regime ($\dot{H} > 0$). (iii) When $0 < H < \sqrt{2\beta} |H_0|$, we obtain an expanding accelerating universe, which is non-singular and lies in the phantom regime. (iv) When $H > \sqrt{2\beta} |H_0|$, the universe begins with a finite time singularity (Big Bang) with a decelerated expansion phase, it matches standard cosmology during the intermediate-time region, then at late times it enters into a non-phantom (since $\dot{H} < 0$) accelerated expansion, and finally in the future the universe results to a de Sitter solution. In this procedure the value of β controls the various transitions points, and in particular the transition from deceleration to acceleration. In particular, a larger β value

corresponds to a later transition to acceleration phase. In summary, this last region is the one that is in agreement with the observed universe evolution.

Having explored the basic features of the phase space portrait of the model at hand, let us extract analytical relations for the deceleration-to-acceleration transition. From Eq. (5.6) we can see that the zero acceleration curve, i.e $\dot{H} = -H^2$, is crossed at

$$H_{tr} = \pm H_0 \sqrt{\frac{\beta(2 + 3w \pm \sqrt{8 + 24w + 9w^2})}{(1 + 3w)}}. \quad (5.7)$$

Focusing on the expanding universe $H > 0$ and assuming the matter to be dust ($w = 0$) we result to the simple relation

$$\beta = \left(\frac{-1 \mp \sqrt{2}}{2} \right) \left(\frac{H_{tr}}{H_0} \right)^2. \quad (5.8)$$

Hence, if the Hubble value at the transition H_{tr} is given accurately from observations then the value of the parameter β can be calculated. In Table 2 we give the estimated values of β according to different choices of H_{tr} (they correspond to $z_{tr} \sim 0.5 - 0.7$ according to observations [4]). The results show that $0.363 \lesssim \beta \lesssim 0.464$ or $-2.707 \lesssim \beta \lesssim -2.117$, which as expected are consistent with the β values that were used in Fig. 9 and were arisen from the requirement $\Omega_{m,0} = 0.318$ (definitely the measurements of $\Omega_{m,0}$ and H_0 are more accurate than the measured of H_{tr}).

z_{tr}	H_{tr} [km/s/Mpc]	β
0.5	~ 100.8	~ -2.117 or 0.363
0.6	~ 107.18	~ -2.394 or 0.411
0.7	~ 113.97	~ -2.707 or 0.464

Table 2. Values of the β parameter of the new model (5.1), and of the corresponding Hubble parameter and redshift at the transition, according to (5.8).

5.3 Cosmological evolution

In this subsection we explore some features of the cosmological evolution in the scenario of the new $f(T)$ model (5.1). First of all, inserting (5.1) into (3.3) and (3.4), using also (2.17), we obtain

$$\rho(H) = \frac{3}{\kappa^2} \left(H^2 - 2\beta H_0^2 \right) e^{\beta \frac{H_0^2}{H^2}}, \quad (5.9)$$

$$p(H) = -\frac{2\dot{H}}{\kappa^2} \left[1 - \beta \left(\frac{H_0}{H} \right)^2 + 2\beta^2 \left(\frac{H_0}{H} \right)^4 \right] e^{\beta \frac{H_0^2}{H^2}} - \rho(H). \quad (5.10)$$

Now since integration of the continuity equation (2.22) in the case of dust matter gives $\rho(H) = \rho_0/a(H)^3$, using (5.9) we obtain the scale factor as a function of the Hubble parameter as

$$a(H) = \left(\frac{\Omega_{m,0} H_0^2}{\Omega_m H^2} \right)^{1/3} = \frac{\Omega_{m,0}^{1/3} H_0^{2/3} e^{-\beta \frac{H_0^2}{3H^2}}}{(H^2 - 2\beta H_0^2)^{1/3}}, \quad (5.11)$$

where $\Omega_m = \frac{\kappa^2 \rho}{3H^2}$ and $\Omega_{m,0}$ its value at present.

In the following we focus on the $\beta > 0$ case, since as we discussed in the phase-space portrait analysis of the previous subsection, it is the one that can lead to a universe evolution in agreement with the observed one. Using (5.11) we obtain the redshift as a function of the Hubble parameter H as

$$z(H) = \left(\frac{H^2 - 2\beta H_0^2}{H_0^2 \Omega_{m,0}} \right)^{1/3} e^{\frac{\beta H_0^2}{3H^2}} - 1. \quad (5.12)$$

The inverse relation of (5.12) gives $H \equiv H(z)$, which can be shown graphically in Fig. 10(a).

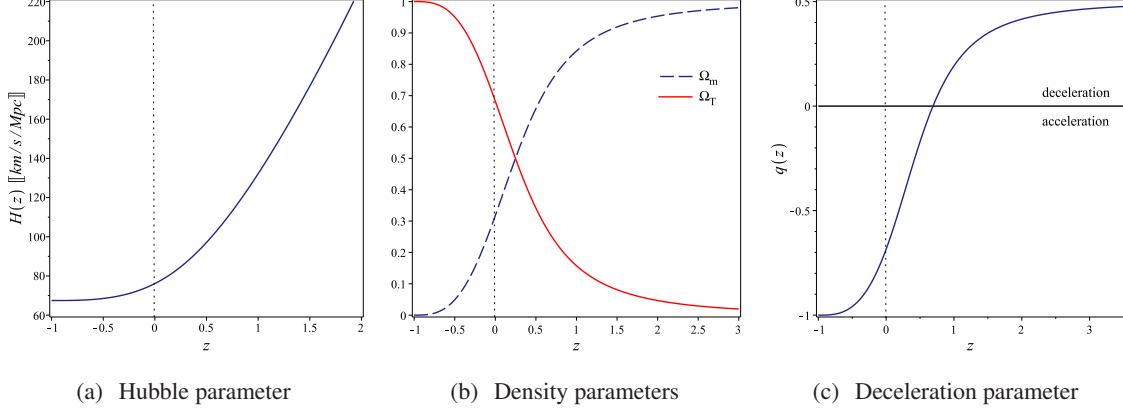


Figure 10. *Cosmological evolution of various quantities, in the new model of (5.1), as a function of the redshift. Left graph: The evolution of the Hubble parameter $H(z)$ from the inverse relation of (5.12). Middle graph: The evolution of the matter and (torsional) dark energy density parameters, $\Omega_m(z)$ and $\Omega_T(z)$, from (5.13) and (5.14) respectively. Right graph: The evolution of the deceleration parameter $q(z)$ from (5.15). We have taken $\beta = 0.393$, and we have set the present values as $H_0 = 76.11$ km/s/Mpc and $\Omega_{m,0} = 0.318$.*

Similarly, from (5.9) we extract the matter density parameter as

$$\Omega_m(H) = \frac{(H^2 - 2\beta H_0^2)}{H^2} e^{\beta \frac{H_0^2}{H^2}}, \quad (5.13)$$

while from (5.2) the (torsional) dark energy density parameter reads as

$$\Omega_T(H) = 1 - \frac{(H^2 - 2\beta H_0^2)}{H^2} e^{\beta \frac{H_0^2}{H^2}}. \quad (5.14)$$

Thus, using the inverse of (5.12), as well as (5.13) and (5.14), in Fig. 10(b) we depict Ω_m and Ω_T as functions of z . The current value of Ω_m is $\Omega_m(z = 0) = \Omega_{m,0} \approx 0.318$, while it approaches unity at larger redshift values. On the other hand, Ω_T is almost zero at large z , while its current value is $\Omega_T(z = 0) \approx 0.682$. These behaviours are in a very good agreement with observations. Additionally, extending the graphs to the far future, namely at $z \rightarrow -1$, we can see that Ω_m drops to zero while $\Omega_T \rightarrow 1$, i.e the universe results in a de Sitter phase.

Concerning the deceleration parameter (2.28), in the case of dust matter using (5.11) it becomes

$$q(H) = \frac{1}{2} \frac{H^4 - 4\beta H_0^2 H^2 - 4\beta^2 H_0^4}{H^4 - \beta H_0^2 H^2 + 2\beta^2 H_0^4}. \quad (5.15)$$

Therefore, using the inverse relation of (5.12) in Fig. 10(c) we present $q(z)$. As we observe, the universe was decelerating at early times, ($q \rightarrow 0.5$ at larger z as expected for a dust-matter dominated phase), it experienced the deceleration-to-acceleration transition at redshift $z_{tr} \approx 0.63$ (in agreement with the expected range $0.6 \lesssim z_{tr} \lesssim 0.8$), and at present it has a value $q(z=0) \approx -0.649$.

Let us now focus on the (torsional) dark energy equation-of-state parameter w_T of (5.4), which using the inverse relation of (5.12) can be expressed as a function of the redshift. In Fig. 11(a) we depict $w_T(z)$ for $\beta = 0.393$, which is consistent with $\Omega_{m,0} = 0.318$ and $H_0 = 76.11$ km/s/Mpc. At large z the graph shows that $w_T(z) \rightarrow -1$, i.e the (torsional) dark energy behaves as a cosmological constant, nevertheless since at the same time $\Omega_T(z)$ is almost zero (see Fig. 10(b)) we do not expect any deviation from standard cosmology and the galaxy formation. However, at smaller redshifts $w_T(z)$ evolves in the phantom regime, still inside the observational bounds [4, 14, 143]. Moreover, at the limit $z \rightarrow -1$, $w_T(z)$ evolves towards -1 , consistently with a dark-energy dominated de Sitter universe.

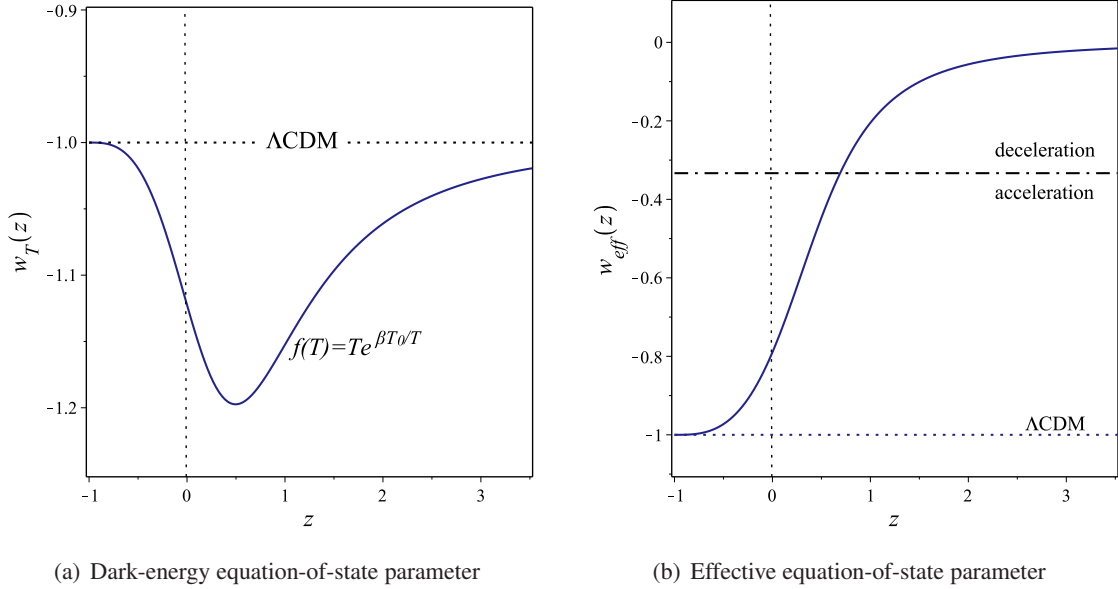


Figure 11. *Left graph: Evolution of the dark energy equation-of-state parameter $w_T(z)$ as a function of the redshift, from (5.4) using the inverse of (5.12), in the new model of (5.1). Right graph: the corresponding evolution of the effective (total) equation-of-state parameter $w_{eff}(z)$, from (5.16) using the inverse of (5.12). We have taken $\beta = 0.393$, and we have set the present values as $H_0 = 76.11$ km/s/Mpc and $\Omega_{m,0} = 0.318$.*

Similarly, let us examine the behaviour of the total equation-of-state parameter of the universe w_{eff} . Inserting (5.6) into (2.27) we can express it as a function of H as

$$w_{eff}(H) = -1 + \frac{(1+w)(H^2 - 2\beta H_0^2)H^2}{(H^4 - \beta H_0^2 H^2 + 2\beta^2 H_0^4)}, \quad (5.16)$$

which for the case of dust matter ($w = 0$) and using the inverse relation of (5.12), can result in a relation $w_{eff}(z)$. In Fig. 11(b) we depict $w_{eff}(z)$ for the same β values with Fig. 11(a). As we observe, w_{eff} behave as dust at large z (as expected during matter domination), it crosses

$w_{eff} = -1/3$ (which corresponds to the deceleration-to-acceleration transition) at redshift $z_{tr} \approx 0.63$, and it drops to $w_{eff}(z) \approx -0.766$ at present ($z = 0$). These behaviours are in agreement with observations [4, 144]. Finally, in the far future, namely at the limit $z \rightarrow -1$, w_{eff} evolves towards -1 , consistently with a de Sitter universe.

Lastly, from the above analysis we have all the materials to estimate the age of the universe

$$t_{age} = - \int_{H_0}^{\infty} \dot{H}^{-1} dH. \quad (5.17)$$

Imposing $H_0 = 76.11$ km/s/Mpc, $\beta = 0.426$ and using the phase portrait of the model at hand, namely (5.6), we find $t_{age} \sim 13.7$ billion years. Although the value $\beta = 0.426$ is consistent with the results of Table 2, the model in this case gives a lower matter density parameter $\Omega_{m,0} \sim 0.227$ as predicted by (5.5). However, by setting $\beta = 0.393$ (which gives $\Omega_{m,0} = 0.318$) and $H_0 = 70$ km/s/Mpc, the model predicts an age of ~ 13.6 billion years. Hence, we conclude that even if the current Hubble constant H_0 and the matter density parameter $\Omega_{m,0}$ have large values, the model can predict an age consistent with the WMAP and Planck results [141].

5.4 Two diagnostic tests

We close this section by performing two diagnostics tests on the new $f(T)$ model proposed in (5.1). The first test is the $Om(z)$ diagnostic test [145], and it is useful in order to resolve the known degeneracy that exists between the dark-energy equation-of-state parameter, which in the present work is of torsional origin, namely w_T , with the dark-matter density parameter Ω_m . The second study concerns the sound speed of the scalar perturbations of the theory.

The $Om(z)$ diagnostic test is a useful tool to distinguish a specific dark energy model amongst others, as well as from the Λ CDM cosmology. The $Om(z)$ diagnostic is defined by [145]

$$Om(z) = \frac{(H(z)/H_0)^2 - 1}{(1+z)^3 - 1}, \quad (5.18)$$

which has less dependence on the matter density parameter and can be determined by the value of H_0 . For Λ CDM paradigm it simply gives a straight line in $(z, Om(z))$ plane, since $H^2 \propto (1+z)^3$, while the dynamical dark energy models lead to curves. In phantom dark energy models ($w_{DE} < -1$), $Om(z)$ has a negative slope, while in models where dark energy lies in the quintessence regime ($w_{DE} > -1$) it has a positive slope.

In the model at hand we can use the inverse relation of (5.12) in order to extract the corresponding $Om(z)$ through (5.18), and in Fig. 12(a) we depict it. This graph confirms that in the present model the torsional dark energy lies in the phantom regime, since the slope is negative. This is in agreement with the combination of Supernovae Type I (SNIa), Baryon Acoustic Oscillations (BAO) and Cosmic Microwave Background (CMB) data at 1σ confidence level [145, 146]. At large z the graph matches Λ CDM cosmology, as we also found in the previous subsections.

Let us now come to the behaviour of scalar perturbations in the theory, since for every gravitational theory it provides an important test for its stability and validity. In viable models the square of the sound speed of these perturbations should be $0 \leq c_s^2 \leq 1$ in order to maintain the causality and stability conditions. For $f(T)$ gravity in an FRW background the squared sound speed of scalar

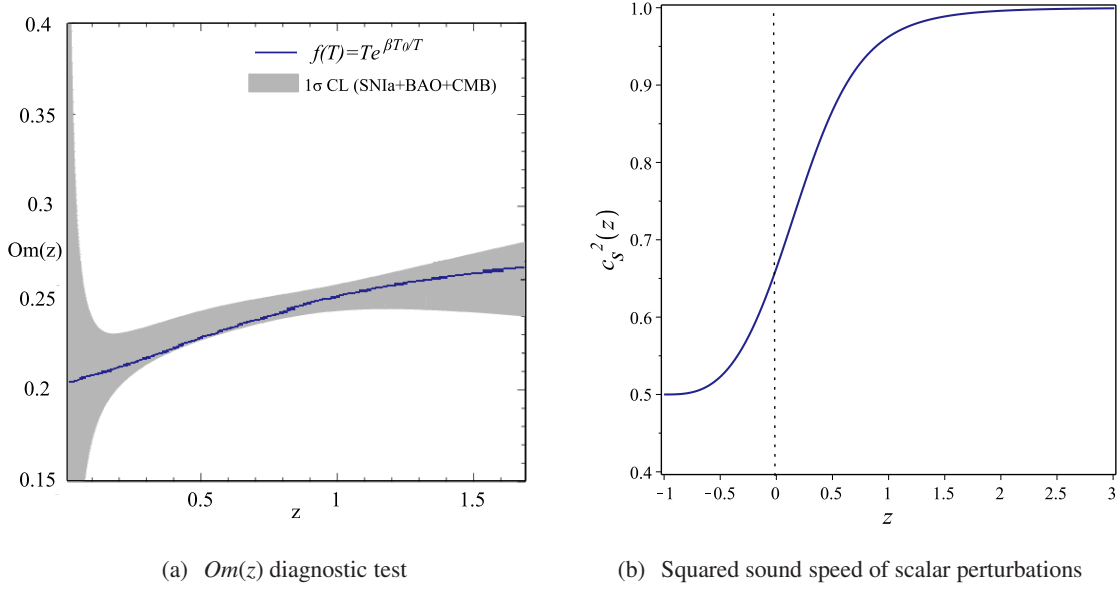


Figure 12. *Left graph: Evolution of the $Om(z)$ parameter (5.18) for the $Om(z)$ diagnostic test, using also the inverse of (5.12), for the new model of (5.1). The gray-shaded region defines the 1σ confidence level fittings using the combined SNIa, BAO and CMB data [145]. Right graph: Evolution of the squared sound speed of the scalar perturbations using (5.20), using also the inverse of (5.12). We have taken $\beta = 0.393$, and we have set the present values as $H_0 = 76.11$ km/s/Mpc and $\Omega_{m,0} = 0.318$.*

perturbation is given by [29, 36]

$$c_s^2 = \frac{f_T}{f_T + 2T f_{TT}}, \quad (5.19)$$

which for the $f(T)$ model (5.1), and using that $T = -6H^2$, it becomes

$$c_s^2(H) = \frac{(H^2 - \beta H_0^2)H^2}{H^4 - \beta H_0^2 H^2 + 2\beta^2 H_0^4}. \quad (5.20)$$

Hence, using the inverse relation of (5.12) we extract $c_s^2(z)$ as a function of the redshift, and we depict it in Fig. 12(b). From this graph it is clear that the sound-speed square is close to 1 (still with $c_s^2 \leq 1$) at large z , then it drops to ≈ 0.66 at present ($z = 0$), while $c_s^2 \rightarrow 0.5$ in the far future $z \rightarrow -1$. Therefore, the model at hand does not suffer from ghost instabilities or acausality at any time of the evolution.

In summary, the $f(T)$ ansatz (5.1) fulfills the basic requirements on both background and perturbation levels, and thus it can be considered as a viable $f(T)$ model.

6 Conclusions

In the present work we used dynamical system methods in order to explore the general behaviour of $f(T)$ cosmology. These methods allow to bypass the complications and non-linearities of the equations in a cosmological scenario, and obtain information about their global behaviour and

dynamics without the need of extracting complete analytical solutions. In contrast to the standard applications of dynamical system methods in given cosmological scenarios, in which one results to a multi-dimensional system whose investigation is in general complicated and it is restricted only to specific forms of the involved functions, in our analysis we presented a way to transform the $f(T)$ cosmological equations into a one-dimensional autonomous system. In particular, we took advantage of the crucial property that the torsion scalar in flat FRW geometry is just a function of the Hubble function H , and thus in a general $f(T)$ cosmological scenario every quantity is expressed as a function of H . Hence, we were able to embed all the information of $f(T)$ cosmology in one phase portrait equation of the form $\dot{H} = \mathcal{F}(H)$.

As a first step, we investigated in detail the phase space portraits that arise from the above equation in the case of general $f(T)$ cosmology, exploring the basic features and possible behaviours. As we showed, $f(T)$ cosmology can describe the universe evolution in agreement with observations, namely starting from a Big Bang singularity, evolving into the subsequent thermal history and the matter domination, entering into a late-time accelerated expansion, and resulting to the de Sitter phase in the far future. Nevertheless, $f(T)$ cosmology exhibits a rich class of more exotic behaviours, such as decelerated and accelerated contraction, cosmological (singular or non-singular) bounce and turnaround, the realization of the phantom-divide crossing, and the appearance of the Big Brake and the Big Crunch. Moreover, it can exhibit various singularities, including the non-harmful ones of type II and type IV.

As a next step, we investigated the phase space portraits of three specific viable $f(T)$ forms, that pass the basic cosmological requirements. Using the advanced method of the one-dimensional analysis, we were able to reproduce the results that were previously extracted in the literature, providing additionally extra information on the different solution branches and possible behaviours, and offering a more complete picture. Using our method, we were able to extract the required bounds on the model parameters in order to obtain the correct early and intermediate behaviour too, apart from the correct late-time asymptotic one. Interestingly enough, we obtained the same parameter bounds with those acquired through detailed observational confrontation.

Taking into account the information obtained from the investigation of the phase space portraits, we presented a new model of $f(T)$ gravity, namely $f(T) = T e^{\beta T_0/T}$, that can lead to a universe in agreement with observations. In particular, this model can describe the required thermal history of the universe, exhibit the deceleration-to-acceleration transition at the expected redshift, and result today in the correct percentage of dark matter and dark energy. Furthermore, the effective dark energy behaves as cosmological constant at large redshifts, while it behaves as phantom in the epoch of late-time acceleration. In the future the universe is attracted by the de Sitter solution, and it is dominated by the torsional dark energy which behaves as cosmological constant. Moreover, concerning the basic cosmological quantities, these are in agreement with their observed values. Finally, we performed the $Om(z)$ diagnostic test, which can differentiate various dark energy models since it has less dependence on the matter density parameter. Additionally, we examined the behaviour of the scalar perturbations in the scenario at hand, and we showed that their sound speed square is always in the interval $0.5 \leq c_s^2 \leq 1$, which fulfills the stability and causality conditions at all times.

In summary, the method of one-dimensional phase space portraits, that is applicable in $f(T)$ cosmology, can reveal the rich structure and the capabilities of the theory. $f(T)$ gravity proves to

be efficient as a candidate for the description of nature.

Acknowledgments

This work is partially supported by the Egyptian Ministry of Scientific Research under project No. 24-2-12. This article is based upon work from COST Action “Cosmology and Astrophysics Network for Theoretical Advances and Training Actions”, supported by COST (European Cooperation in Science and Technology). ENS wishes to thank Institut de Physique Théorique, Université Paris-Saclay and Laboratoire de Physique Théorique, Univ. Paris-Sud, Université Paris-Saclay, for the hospitality during the last stages of this project.

References

- [1] COBE collaboration, G. F. Smoot et al., *Structure in the COBE differential microwave radiometer first year maps*, *Astrophys. J.* **396** (1992) L1–L5.
- [2] D. N. Spergel, L. Verde, H. V. Peiris, E. Komatsu, M. R. Nolta, C. L. Bennett et al., *First-Year Wilkinson Microwave Anisotropy Probe (WMAP) Observations: Determination of Cosmological Parameters*, *Astrophys. J. S.* **148** (Sept., 2003) 175–194, [[astro-ph/0302209](#)].
- [3] C. L. Bennett, D. Larson, J. L. Weiland, N. Jarosik, G. Hinshaw, N. Odegard et al., *Nine-year Wilkinson Microwave Anisotropy Probe (WMAP) Observations: Final Maps and Results*, *Astrophys. J.* **208** (Oct., 2013) 20, [[1212.5225](#)].
- [4] PLANCK collaboration, P. A. R. Ade et al., *Planck 2015 results. XX. Constraints on inflation*, *Astron. Astrophys.* **594** (2016), [[1502.02114](#)].
- [5] PLANCK collaboration, R. Adam et al., *Planck 2015 results. I. Overview of products and scientific results*, *Astron. Astrophys.* **594** (2016), [[1502.01582](#)].
- [6] V. C. Rubin, N. Thonnard and W. K. Ford, Jr., *Extended rotation curves of high-luminosity spiral galaxies. IV - Systematic dynamical properties, SA through SC*, *Astrophys. J. L.* **225** (Nov., 1978) L107–L111.
- [7] S. M. Faber and J. S. Gallagher, *Masses and mass-to-light ratios of galaxies*, *Annual review of astronomy and astrophysics* **17** (1979) 135–187.
- [8] D. Fabricant, M. Lecar and P. Gorenstein, *X-ray measurements of the mass of M87*, *Astrophys. J.* **241** (Oct., 1980) 552–560.
- [9] A. G. Riess, A. V. Filippenko, P. Challis, A. Clocchiatti, A. Diercks, P. M. Garnavich et al., *Observational Evidence from Supernovae for an Accelerating Universe and a Cosmological Constant*, *The Astronomical Journal* **116** (Sept., 1998) 1009–1038, [[astro-ph/9805201](#)].
- [10] S. Perlmutter, G. Aldering, G. Goldhaber, R. A. Knop, P. Nugent, P. G. Castro et al., *Measurements of Ω and Λ from 42 High-Redshift Supernovae*, *Astrophys. J.* **517** (June, 1999) 565–586, [[astro-ph/9812133](#)].
- [11] O. Farooq, F. R. Madiyar, S. Crandall and B. Ratra, *Hubble Parameter Measurement Constraints on the Redshift of the Deceleration-acceleration Transition, Dynamical Dark Energy, and Space Curvature*, *Astrophys. J.* **835** (2017) 26, [[1607.03537](#)].
- [12] E. Di Valentino, *Crack in the cosmological paradigm*, *Nat. Astron.* **1** (2017) 569, [[1709.04046](#)].

- [13] W. L. Freedman, *Cosmology at at Crossroads: Tension with the Hubble Constant*, *Nat. Astron.* **1** (2017) 0169, [[1706.02739](#)].
- [14] E. Di Valentino, A. Melchiorri and J. Silk, *Reconciling Planck with the local value of H_0 in extended parameter space*, *Phys. Lett. B* **761** (2016) 242–246, [[1606.00634](#)].
- [15] G.-B. Zhao et al., *Dynamical dark energy in light of the latest observations*, *Nat. Astron.* **1** (2017) 627–632, [[1701.08165](#)].
- [16] E. Di Valentino, A. Melchiorri, E. V. Linder and J. Silk, *Constraining Dark Energy Dynamics in Extended Parameter Space*, *Phys. Rev. D* **96** (2017) 023523, [[1704.00762](#)].
- [17] E. J. Copeland, M. Sami and S. Tsujikawa, *Dynamics of dark energy*, *Int. J. Mod. Phys.* (2006) 1753–1936, [[hep-th/0603057](#)].
- [18] Y.-F. Cai, E. N. Saridakis, M. R. Setare and J.-Q. Xia, *Quintom Cosmology: Theoretical implications and observations*, *Phys. Rept.* **493** (2010) 1–60, [[0909.2776](#)].
- [19] S. Nojiri and S. D. Odintsov, *Introduction to modified gravity and gravitational alternative for dark energy*, *eConf* (2006) 06, [[hep-th/0601213](#)].
- [20] S. Capozziello and M. De Laurentis, *Extended Theories of Gravity*, *Phys. Rept.* **509** (2011) 167–321, [[1108.6266](#)].
- [21] Y.-F. Cai, S. Capozziello, M. De Laurentis and E. N. Saridakis, *$f(T)$ teleparallel gravity and cosmology*, *Rept. Prog. Phys.* **79** (2016) 106901, [[1511.07586](#)].
- [22] R. Aldrovandi and J. G. Pereira, *Teleparallel Gravity*, vol. 173. Springer Science+Business Media Dordrecht, 2013, [10.1007/978-94-007-5143-9](#).
- [23] G. R. Bengochea and R. Ferraro, *Dark torsion as the cosmic speed-up*, *Phys. Rev. D* **79** (2009) 124019, [[0812.1205](#)].
- [24] E. V. Linder, *Einstein’s Other Gravity and the Acceleration of the Universe*, *Phys. Rev. D* **81** (2010) 127301, [[1005.3039](#)].
- [25] R. Ferraro and F. Fiorini, *Modified teleparallel gravity: Inflation without inflaton*, *Phys. Rev. D* **75** (2007) 084031, [[gr-qc/0610067](#)].
- [26] R. Ferraro and F. Fiorini, *On Born-Infeld Gravity in Weitzenbock spacetime*, *Phys. Rev. D* **78** (2008) 124019, [[0812.1981](#)].
- [27] K. Bamba, S. Nojiri and S. D. Odintsov, *Trace-anomaly driven inflation in $f(T)$ gravity and in minimal massive bigravity*, *Phys. Lett. B* **731** (2014) 257–264, [[1401.7378](#)].
- [28] K. Bamba, S. D. Odintsov and E. N. Saridakis, *Inflationary cosmology in unimodular $F(T)$ gravity*, *Mod. Phys. Lett. A* **32** (2017) 1750114, [[1605.02461](#)].
- [29] S.-H. Chen, J. B. Dent, S. Dutta and E. N. Saridakis, *Cosmological perturbations in $f(T)$ gravity*, *Phys. Rev. D* **83** (2011) 023508, [[1008.1250](#)].
- [30] P. Yu. Tsyba, I. I. Kulnazarov, K. K. Yerzhanov and R. Myrzakulov, *Pure kinetic k -essence as the cosmic speed-up*, *Int. J. Theor. Phys.* **50** (2011) 1876–1886, [[1008.0779](#)].
- [31] R.-J. Yang, *New types of $f(T)$ gravity*, *Eur. Phys. J. C* **71** (2011) 1797, [[1007.3571](#)].
- [32] K. Bamba, C.-Q. Geng and C.-C. Lee, *Comment on ‘Einstein’s Other Gravity and the Acceleration of the Universe’*, [1008.4036](#).
- [33] R. Myrzakulov, *$F(T)$ gravity and k -essence*, *Gen. Rel. Grav.* **44** (Dec., 2012) 3059–3080, [[1008.4486](#)].

- [34] K. Bamba, C.-Q. Geng, C.-C. Lee and L.-W. Luo, *Equation of state for dark energy in $f(T)$ gravity*, *JCAP* **1101** (2011) 021, [[1011.0508](#)].
- [35] J. B. Dent, S. Dutta and E. N. Saridakis, *$f(T)$ gravity mimicking dynamical dark energy. Background and perturbation analysis*, *JCAP* **1101** (2011) 009, [[1010.2215](#)].
- [36] Y.-F. Cai, S.-H. Chen, J. B. Dent, S. Dutta and E. N. Saridakis, *Matter Bounce Cosmology with the $f(T)$ Gravity*, *Class. Quant. Grav.* **28** (2011) 215011, [[1104.4349](#)].
- [37] M. Sharif and S. Rani, *$F(T)$ Models within Bianchi Type I Universe*, *Mod. Phys. Lett. A* **26** (2011) 1657–1671, [[1105.6228](#)].
- [38] H. Wei, H.-Y. Qi and X.-P. Ma, *Constraining $f(T)$ Theories with the Varying Gravitational Constant*, *Eur. Phys. J. C* **72** (2012) 2117, [[1108.0859](#)].
- [39] P. Wu and H. Yu, *The Stability of the Einstein static state in $f(T)$ gravity*, *Phys. Lett. B* **703** (2011) 223–227, [[1108.5908](#)].
- [40] K. Karami, A. Abdolmaleki, S. Asadzadeh and Z. Safari, *Holographic $f(T)$ -gravity model with power-law entropy correction*, *Phys. Rev. D* **88** (2013) 084034, [[1111.7269](#)].
- [41] M. Jamil, D. Momeni, N. S. Serikbayev and R. Myrzakulov, *FRW and Bianchi type I cosmology of f -essence*, *Astrophys. Space Sci.* **339** (May, 2012) 37–43, [[1112.4472](#)].
- [42] K. Karami, A. Abdolmaleki, S. Asadzadeh and Z. Safari, *QCD ghost $f(T)$ -gravity model*, *Eur. Phys. J. C* **73** (2013) 2565, [[1202.2278](#)].
- [43] M. R. Setare and M. J. S. Houndjo, *Finite-time future singularities models in $f(T)$ gravity and the effects of viscosity*, *Can. J. Phys.* **91** (2013) 260–267, [[1203.1315](#)].
- [44] H. Dong, Y.-b. Wang and X.-h. Meng, *Extended Birkhoff's Theorem in the $f(T)$ Gravity*, *Eur. Phys. J. C* **72** (2012) 2002, [[1203.5890](#)].
- [45] N. Tamanini and C. G. Boehmer, *Good and bad tetrads in $f(T)$ gravity*, *Phys. Rev. D* **86** (2012) 044009, [[1204.4593](#)].
- [46] M. E. Rodrigues, M. H. Daouda, M. J. S. Houndjo, R. Myrzakulov and M. Sharif, *Inhomogeneous Universe in $f(T)$ Theory*, *Grav. Cosmol.* **20** (2014) 80–89, [[1205.0565](#)].
- [47] A. Banijamali and B. Fazlpour, *Tachyonic Teleparallel Dark Energy*, *Astrophys. Space Sci.* **342** (2012) 229–235, [[1206.3580](#)].
- [48] F. Darabi, *Reconstruction of $f(R)$, $f(T)$ and $f(G)$ models inspired by variable deceleration parameter*, *Astrophys. Space Sci.* **343** (2013) 499–504, [[1207.0212](#)].
- [49] D. Liu and M. J. Reboucas, *Energy conditions bounds on $f(T)$ gravity*, *Phys. Rev. D* **86** (2012) 083515, [[1207.1503](#)].
- [50] M. R. Setare and N. Mohammadipour, *Cosmological viability conditions for $f(T)$ dark energy models*, *JCAP* **1211** (2012) 030, [[1211.1375](#)].
- [51] V. F. Cardone, N. Radicella and S. Camera, *Accelerating $f(T)$ gravity models constrained by recent cosmological data*, *Phys. Rev.* (2012) 124007, [[1204.5294](#)].
- [52] S. Chattopadhyay and A. Pasqua, *Reconstruction of $f(T)$ gravity from the Holographic Dark Energy*, *Astrophys. Space Sci.* **344** (Mar., 2013) 269–274, [[1211.2707](#)].
- [53] K. Bamba, J. de Haro and S. D. Odintsov, *Future Singularities and Teleparallelism in Loop Quantum Cosmology*, *JCAP* **1302** (2013) 008, [[1211.2968](#)].
- [54] M. R. Setare and N. Mohammadipour, *Can $f(T)$ gravity theories mimic Λ CDM cosmic history*,

- [JCAP **1301** \(2013\) 015](#), [[1301.4891](#)].
- [55] J.-T. Li, C.-C. Lee and C.-Q. Geng, *Einstein Static Universe in Exponential $f(T)$ Gravity*, [Eur. Phys. J. C **73** \(2013\) 2315](#), [[1302.2688](#)].
- [56] S. Camera, V. F. Cardone and N. Radicella, *Detectability of Torsion Gravity via Galaxy Clustering and Cosmic Shear Measurements*, [Phys. Rev. \(2014\) 083520](#), [[1311.1004](#)].
- [57] K. Bamba, S. Nojiri and S. D. Odintsov, *Effective $F(T)$ gravity from the higher-dimensional Kaluza-Klein and Randall-Sundrum theories*, [Phys. Lett. B **725** \(2013\) 368–371](#), [[1304.6191](#)].
- [58] S. Basilakos, S. Capozziello, M. De Laurentis, A. Paliathanasis and M. Tsamparlis, *Noether symmetries and analytical solutions in $f(T)$ -cosmology: A complete study*, [Phys. Rev. D **88** \(2013\) 103526](#), [[1311.2173](#)].
- [59] J.-Z. Qi, R.-J. Yang, M.-J. Zhang and W.-B. Liu, *Transient acceleration in $f(T)$ gravity*, [Res. Astron. Astrophys. **16** \(2016\) 022](#), [[1403.7287](#)].
- [60] G. G. L. Nashed, *Exact homogenous anisotropic solution in $f(t)$ gravity theory*, [Eur. Phys. J. P **129** \(Sep, 2014\) 188](#).
- [61] F. Darabi, M. Mousavi and K. Atazadeh, *Geodesic deviation equation in $f(T)$ gravity*, [Phys. Rev. D **91** \(2015\) 084023](#), [[1501.00103](#)].
- [62] G. L. Nashed, *FRW in quadratic form of $f(T)$ gravitational theories*, [Gen. Rel. Grav. **47** \(2015\) 75](#), [[1506.08695](#)].
- [63] V. Fayaz, H. Hossienkhani, A. Pasqua, M. Amirabadi and M. Ganji, *$f(t)$ theories from holographic dark energy models within bianchi type i universe*, [The European Physical Journal Plus **130** \(Feb, 2015\) 28](#).
- [64] H. Abedi and M. Salti, *Multiple field modified gravity and localized energy in teleparallel framework*, [Gen. Rel. Grav. **47** \(Jul, 2015\) 93](#).
- [65] M. Krššák and E. N. Saridakis, *The covariant formulation of $f(T)$ gravity*, [Class. Quant. Grav. **33** \(2016\) 115009](#), [[1510.08432](#)].
- [66] S. Pan, J. de Haro, A. Paliathanasis, R. J. Slagter and S. R. J., *Evolution and Dynamics of a Matter creation model*, [Mon. Not. Roy. Astron. Soc. **460** \(2016\) 1445–1456](#), [[1601.03955](#)].
- [67] A. Paliathanasis, J. D. Barrow and P. G. L. Leach, *Cosmological Solutions of $f(T)$ Gravity*, [Phys. Rev. D **94** \(2016\) 023525](#), [[1606.00659](#)].
- [68] C.-Q. Geng, C.-C. Lee, E. N. Saridakis and Y.-P. Wu, *Teleparallel dark energy*, [Phys. Lett. B **704** \(2011\) 384–387](#), [[1109.1092](#)].
- [69] C. Xu, E. N. Saridakis and G. Leon, *Phase-Space analysis of Teleparallel Dark Energy*, [JCAP **1207** \(2012\) 005](#), [[1202.3781](#)].
- [70] G. Kofinas and E. N. Saridakis, *Teleparallel equivalent of Gauss-Bonnet gravity and its modifications*, [Phys. Rev. D **90** \(2014\) 084044](#), [[1404.2249](#)].
- [71] J. Haro and J. Amoros, *Viability of the matter bounce scenario in $F(T)$ gravity and Loop Quantum Cosmology for general potentials*, [JCAP **1412** \(2014\) 031](#), [[1406.0369](#)].
- [72] W. El Hanafy and G. G. L. Nashed, *The hidden flat like universe*, [Eur. Phys. J. C **75** \(2015\) 279](#), [[1409.7199](#)].
- [73] M. Sharif and A. Sehrish, *Dark Energy Models and Cosmic Acceleration with Anisotropic Universe in $f(T)$ Gravity*, [Communications in Theoretical Physics **61** \(Apr., 2014\) 482–490](#).

- [74] W. El Hanafy and G. G. L. Nashed, *The hidden flat like universe II: Quasi inverse power law inflation by $f(T)$ gravity*, *Astrophys. Space Sci.* **361** (2016) 266, [1510.02337].
- [75] S. Capozziello, O. Luongo and E. N. Saridakis, *Transition redshift in $f(T)$ cosmology and observational constraints*, *Phys. Rev. D* **91** (2015) 124037, [1503.02832].
- [76] R. C. Nunes, S. Pan and E. N. Saridakis, *New observational constraints on $f(T)$ gravity from cosmic chronometers*, *JCAP* **1608** (2016) 011, [1606.04359].
- [77] R. C. Nunes, A. Bonilla, S. Pan and E. N. Saridakis, *Observational Constraints on $f(T)$ gravity from varying fundamental constants*, *Eur. Phys. J. C* **77** (2017) 230, [1608.01960].
- [78] J.-Z. Qi, S. Cao, M. Biesiada, X. Zheng and H. Zhu, *New observational constraints on $f(T)$ cosmology from radio quasars*, *Eur. Phys. J. C* **77** (2017) 502, [1708.08603].
- [79] A. Awad, W. El Hanafy, G. G. L. Nashed, S. D. Odintsov and V. K. Oikonomou, *Constant-roll Inflation in $f(T)$ Teleparallel Gravity*, 1710.00682.
- [80] V. K. Oikonomou, *Viability of the intermediate inflation scenario with $F(T)$ gravity*, *Phys. Rev. D* **95** (2017) 084023, [1703.10515].
- [81] A. Jawad, S. Rani and M. Saleem, *Cosmological study of reconstructed $f(T)$ models*, *Astrophys. Space Sci.* **362** (Apr., 2017) 63.
- [82] S. Capozziello, G. Lambiase and E. N. Saridakis, *Constraining $f(T)$ teleparallel gravity by Big Bang Nucleosynthesis*, *Eur. Phys. J. C* **77** (2017) 576, [1702.07952].
- [83] L. Karpathopoulos, S. Basilakos, G. Leon, A. Paliathanasis and M. Tsamparlis, *Cartan symmetries and global dynamical systems analysis in a higher-order modified teleparallel theory*, 1709.02197.
- [84] R.-X. Miao, M. Li and Y.-G. Miao, *Violation of the first law of black hole thermodynamics in $f(T)$ gravity*, *JCAP* **1111** (2011) 033, [1107.0515].
- [85] S. Capozziello, P. A. Gonzalez, E. N. Saridakis and Y. Vasquez, *Exact charged black-hole solutions in D -dimensional $f(T)$ gravity: torsion vs curvature analysis*, *JHEP* **02** (2013) 039, [1210.1098].
- [86] J. Bhadra and U. Debnath, *Primordial Black Holes Evolution in $f(T)$ Gravity*, *International Journal of Theoretical Physics* (Oct., 2013) .
- [87] M. E. Rodrigues, M. J. S. Houndjo, D. Momeni and R. Myrzakulov, *Planar Symmetry in $f(T)$ Gravity*, *International Journal of Modern Physics D* **22** (July, 2013) 1350043, [1302.4372].
- [88] J. Aftergood and A. DeBenedictis, *Matter conditions for regular black holes in $f(T)$ gravity*, *Phys. Rev. D* **90** (2014) 124006, [1409.4084].
- [89] A. Paliathanasis, S. Basilakos, E. N. Saridakis, S. Capozziello, K. Atazadeh, F. Darabi et al., *New Schwarzschild-like solutions in $f(T)$ gravity through Noether symmetries*, *Phys. Rev. D* **89** (2014) 104042, [1402.5935].
- [90] G. G. L. Nashed, *Kerr-Newman-NUT Black Hole in $f(T)$ Gravity Theory and Its Thermodynamical Quantities*, *Journal of the Physical Society of Japan* **84** (Apr., 2015) 044006.
- [91] E. L. B. Junior, M. E. Rodrigues and M. J. S. Houndjo, *Born-Infeld and Charged Black Holes with non-linear source in $f(T)$ Gravity*, *JCAP* **1506** (2015) 037, [1503.07427].
- [92] G. G. L. Nashed, *Kerr-NUT black hole thermodynamics in $f(T)$ gravity theories*, *European Physical Journal Plus* **130** (July, 2015) 124.
- [93] E. L. B. Junior, M. E. Rodrigues and M. J. S. Houndjo, *Regular black holes in $f(T)$ Gravity through*

- a nonlinear electrodynamics source, *JCAP* **1510** (2015) 060, [[1503.07857](#)].
- [94] G. G. L. Nashed and W. El Hanafy, *Analytic rotating black hole solutions in N -dimensional $f(T)$ gravity*, *Eur. Phys. J. C* **77** (2017) 90, [[1612.05106](#)].
- [95] A. K. Ahmed, M. Azreg-Anou, S. Bahamonde, S. Capozziello and M. Jamil, *Astrophysical flows near $f(T)$ gravity black holes*, *Eur. Phys. J. C* **76** (2016) 269, [[1602.03523](#)].
- [96] M. E. Rodrigues and E. L. B. Junior, *Spherical Accretion of Matter by Charged Black Holes on $f(T)$ Gravity*, [1606.04918](#).
- [97] G. G. L. Nashed, *(1+4)-dimensional spherically symmetric black holes in $f(T)$* , *Gravitation and Cosmology* **23** (Jan., 2017) 63–69.
- [98] Z.-F. Mai and H. Lu, *Black Holes, Dark Wormholes and Solitons in $f(T)$ Gravities*, *Phys. Rev. D* **95** (2017) 124024, [[1704.05919](#)].
- [99] A. M. Awad, S. Capozziello and G. G. L. Nashed, *D -dimensional charged Anti-de-Sitter black holes in $f(T)$ gravity*, *JHEP* **07** (2017) 136, [[1706.01773](#)].
- [100] S. Capozziello, R. D’Agostino and O. Luongo, *Model-independent reconstruction of $f(T)$ teleparallel cosmology*, *General Relativity and Gravitation* **49** (2017) 141, [[1706.02962](#)].
- [101] E. J. Copeland, A. R. Liddle and D. Wands, *Exponential potentials and cosmological scaling solutions*, *Phys. Rev. D* **57** (1998) 4686–4690, [[gr-qc/9711068](#)].
- [102] P. G. Ferreira and M. Joyce, *Structure formation with a selftuning scalar field*, *Phys. Rev. Lett.* **79** (1997) 4740–4743, [[astro-ph/9707286](#)].
- [103] A. A. C. (auth.), *Dynamical Systems and Cosmology*, vol. 291 of *Astrophysics and Space Science Library*. Springer Netherlands, 1 ed., 2003, [10.1007/978-94-017-0327-7](#).
- [104] G. Leon and C. R. Fadrakas, *Cosmological dynamical systems*. LAP Lambert Academic Publishing, 2012.
- [105] A. A. Coley, ed., *Dynamical Systems and Cosmology*, vol. 291 of *Astrophysics and Space Science Library*, Oct., 2003. [10.1007/978-94-017-0327-7](#).
- [106] J. Wainwright and G. F. R. Ellis, *Dynamical Systems in Cosmology*. Cambridge University Press, June, 2005, [10.1017/CBO9780511524660](#).
- [107] X.-m. Chen, Y.-g. Gong and E. N. Saridakis, *Phase-space analysis of interacting phantom cosmology*, *JCAP* **0904** (2009) 001, [[0812.1117](#)].
- [108] A. Awad, *Fixed points and FLRW cosmologies: Flat case*, *Phys. Rev. D* **87** (May, 2013) 103001, [[1303.2014](#)].
- [109] C. G. Boehmer and N. Chan, *Dynamical systems in cosmology*, [1409.5585](#).
- [110] G. Kofinas, G. Leon and E. N. Saridakis, *Dynamical behavior in $f(T, T_G)$ cosmology*, *Class. Quant. Grav.* **31** (2014) 175011, [[1404.7100](#)].
- [111] S. D. Odintsov, V. K. Oikonomou and P. V. Tretyakov, *Phase space analysis of the accelerating multifluid Universe*, *Phys. Rev. D* **96** (2017) 044022, [[1707.08661](#)].
- [112] P. Wu and H. W. Yu, *The dynamical behavior of $f(T)$ theory*, *Phys. Lett. B* **692** (2010) 176–179, [[1007.2348](#)].
- [113] M. A. Skugoreva, E. N. Saridakis and A. V. Toporensky, *Dynamical features of scalar-torsion theories*, *Phys. Rev. D* **91** (2015) 044023, [[1412.1502](#)].

- [114] S. Carloni, F. S. N. Lobo, G. Otalora and E. N. Saridakis, *Dynamical system analysis for a nonminimal torsion-matter coupled gravity*, *Phys. Rev. D* **93** (2016) 024034, [[1512.06996](#)].
- [115] K. Bamba, G. G. L. Nashed, W. El Hanafy and S. K. Ibraheem, *Bounce inflation in $f(T)$ Cosmology: A unified inflaton-quintessence field*, *Phys. Rev. D* **94** (2016) 083513, [[1604.07604](#)].
- [116] A. Awad and G. Nashed, *Generalized teleparallel cosmology and initial singularity crossing*, *JCAP* **1702** (2017) 046, [[1701.06899](#)].
- [117] W. El Hanafy and G. G. L. Nashed, *Lorenz Gauge Fixing of $f(T)$ Teleparallel Cosmology*, *Int. J. Mod. Phys. D* **26** (2017) 1750154, [[1707.01802](#)].
- [118] W. El Hanafy and G. G. L. Nashed, *Generic Phase Portrait Analysis of the Finite-time Singularities and Generalized Teleparallel Gravity*, *Chin. Phys.* (2017) 125103, [[1702.05786](#)].
- [119] M. Hohmann, L. Jarv and U. Ualikhanova, *Dynamical systems approach and generic properties of $f(T)$ cosmology*, *Phys. Rev. D* **96** (2017) 043508, [[1706.02376](#)].
- [120] B. Mirza and F. Oboudiat, *Constraining $f(T)$ gravity by dynamical system analysis*, [1704.02593](#).
- [121] G. R. Bengochea and R. Ferraro, *Dark torsion as the cosmic speed-up*, *Phys. Rev. D* **79** (June, 2009) 124019, [[0812.1205](#)].
- [122] E. V. Linder, *Einstein's other gravity and the acceleration of the Universe*, *Phys. Rev. D* **81** (June, 2010) 127301, [[1005.3039](#)].
- [123] M. Li, R.-X. Miao and Y.-G. Miao, *Degrees of freedom of $f(T)$ gravity*, *JHEP* **07** (2011) 108, [[1105.5934](#)].
- [124] S. H. Strogatz, *Nonlinear Dynamics And Chaos: With Applications To Physics, Biology, Chemistry And Engineering*, vol. 1 of *Studies in Nonlinearity*. 1994.
- [125] S. Nojiri, S. D. Odintsov and S. Tsujikawa, *Properties of singularities in (phantom) dark energy universe*, *Phys. Rev. D* **71** (2005) 063004, [[hep-th/0501025](#)].
- [126] J. D. Barrow, G. J. Galloway and F. J. Tipler, *The closed-universe recollapse conjecture*, *Mon. Not. Roy. Astr. Soc.* **223** (Dec., 1986) 835–844.
- [127] J. D. Barrow, *Sudden future singularities*, *Class. Quant. Grav.* **21** (2004) L79–L82, [[gr-qc/0403084](#)].
- [128] Z. Keresztes, L. A. Gergely and A. Yu. Kamenshchik, *The paradox of soft singularity crossing and its resolution by distributional cosmological quantities*, *Phys. Rev. D* **86** (2012) 063522, [[1204.1199](#)].
- [129] A. Awad, *Weyl Anomaly and Initial Singularity Crossing*, *Phys. Rev. D* **93** (2016) 084006, [[1512.06405](#)].
- [130] Y.-F. Cai and E. N. Saridakis, *Non-singular Cyclic Cosmology without Phantom Menace*, *J. Cosmol.* **17** (2011) 7238–7254, [[1108.6052](#)].
- [131] S. Nojiri and E. N. Saridakis, *Phantom without ghost*, *Astrophys. Space Sci.* **347** (2013) 221–226, [[1301.2686](#)].
- [132] M. Novello and S. E. P. Bergliaffa, *Bouncing Cosmologies*, *Phys. Rept.* **463** (2008) 127–213, [[0802.1634](#)].
- [133] Y.-F. Cai and E. N. Saridakis, *Non-singular cosmology in a model of non-relativistic gravity*, *JCAP* **0910** (2009) 020, [[0906.1789](#)].
- [134] L. Fernández-Jambrina and R. Lazkoz, *Geodesic Completeness around Sudden Singularities*, in *A*

Century of Relativity Physics: ERE 2005 (L. Mornas and J. Diaz Alonso, eds.), vol. 841 of *American Institute of Physics Conference Series*, pp. 420–423, June, 2006, [0903.5529](#), [DOI](#).

- [135] L. Fernández-Jambrina and R. Lazkoz, *Classification of cosmological milestones*, *Phys. Rev. D* **74** (Sept., 2006) 064030, [[gr-qc/0607073](#)].
- [136] J. D. Barrow and S. Cotsakis, *Geodesics at sudden singularities*, *Phys. Rev. D* **88** (Sept., 2013) 067301, [[1307.5005](#)].
- [137] A. Kamenshchik, Z. Keresztes and L. A. Gergely, *The paradox of soft singularity crossing avoided by distributional cosmological quantities*, in *Proceedings, 13th Marcel Grossmann Meeting on Recent Developments in Theoretical and Experimental General Relativity, Astrophysics, and Relativistic Field Theories (MG13): Stockholm, Sweden, July 1-7, 2012*, 2015.
- [138] L. A. Gergely, Z. Keresztes and A. Yu. Kamenshchik, *Distributional cosmological quantities solve the paradox of soft singularity crossing*, *AIP Conf. Proc.* **1514** (2013) 132–135, [[1304.1415](#)].
- [139] S. Nesseris, S. Basilakos, E. N. Saridakis and L. Perivolaropoulos, *Viable $f(T)$ models are practically indistinguishable from Λ CDM*, *Phys. Rev. D* **88** (2013) 103010, [[1308.6142](#)].
- [140] L. Iorio and E. N. Saridakis, *Solar system constraints on $f(T)$ gravity*, *Mon. Not. Roy. Astron. Soc.* **427** (2012) 1555, [[1203.5781](#)].
- [141] PLANCK collaboration, P. A. R. Ade et al., *Planck 2015 results. XIII. Cosmological parameters*, *Astron. Astrophys.* **594** (2016), [[1502.01589](#)].
- [142] K. Bamba, C.-Q. Geng, C.-C. Lee and L.-W. Luo, *Equation of state for dark energy in $f(T)$ gravity*, *J. Cosmo. Astropart. Phys.* **1** (Jan., 2011) 21, [[1011.0508](#)].
- [143] J. Cepa, *Constraints on the cosmic equation of state: Age conflict versus phantom energy. Age - redshift relations in an accelerated universe*, *Astron. Astrophys.* **422** (2004) 831–839, [[astro-ph/0403616](#)].
- [144] A. Mukherjee, *Acceleration of the universe: a reconstruction of the effective equation of state*, *Mon. Not. Roy. Astron. Soc.* **460** (2016) 273–282, [[1605.08184](#)].
- [145] V. Sahni, A. Shafieloo and A. A. Starobinsky, *Two new diagnostics of dark energy*, *Phys. Rev. D* **78** (2008) 103502, [[0807.3548](#)].
- [146] A. I. Lonappan, Ruchika and A. A. Sen, *Is it time to go beyond Λ CDM universe?*, [1705.07336](#).